BIFURCATION AND COLLAPSE ANALYSIS OF STRINGER AND RING-STRINGER STIFFENED CYLINDRICAL SHELLS WITH CUTOUTS

by

A. N. Palazotto
Associate Professor (Structures)
Mechanics & Engineering Systems Department
Air Force Institute of Technology, WPAFB
Dayton, OH 45433

ABSTRACT

This paper presents results for cylindric .l shell configurations using the STAGS computer program. Discontinuities have been imposed upon the shell's skin by incorporating symmetrical cutout openings. In addition, the surface is stiffened with both stringer and ring-stringer arrangements.

The cutout problem has been shown to be highly nonlinear for smooth surface shells, but the author has found that bifurcation and collapse loads are close when one is considering stiffened skin configurations. In order to arrive at this conclusion, it was necessary to evaluate the following:

- comparison between smeared and discrete stiffener theory for linear solutions
- numerical finite difference convergence as directed toward buckling determination
- collapse load results with the various skin stiffeners.

This paper also includes a linear bifurcation study relating to stiffening effects around cutout areas present within stringer and ring-stringer shell surfaces. Comparisons have been made between a variety of geometric positions considering cutout frame and thickened skin additions. The investigation points toward an optimum positioning.

NOMENCLATURE

$2a$ = cutout dimension

A_1, A_2 = cross sectional area of stringer and ring

b_1, b_2 = spacing of stringer and rings

E = modulus of elasticity

GJ = torsional stiffness

h, t = shell thickness

I_y, I_1 = moment of inertia of stringer

L = length of shell

N_{xy} = resultant shear force per unit length

n = number of nodes in finite difference scheme

P_{cr} = bifurcation load

P_o = bifurcation load for shell with no cutout

R = radius of shell

u, v, w = displacement in x, y and radial direction

x, y, θ = coordinates

Z = Batdorf shell parameter $(1 - \nu^2)^{\frac{1}{2}}(L/R)^2(R/h)$

β = slope of deflected surface at boundary

ν = Poisson's ratio

INTRODUCTION

It is obvious the cylindrical shell is an important structural configuration within the aerospace industry. One finds an unlimited amount of research papers directed toward this common shell surface. Yet, the practical consideration of skin cutouts and their stiffening has, for the most part, presented certain amounts of analytical difficulties. Until recently, the stiffening of these cutouts became an experimental trial and error procedure [1]. It is now possible to

obtain a computational evaluation of cutout effects and reinforcements using an all purpose shell program developed by Lockheed. This program has been named STAGS (Structural Analysis of General Shells). It contains the overall capabilities of either nonlinear or linear shell analysis leading to bifurcation or collapse loads for several different shell geometries, in particular cylindrical shells [2, 3, 4, 5].

Studies have shown that a shell buckling resistance is increased with the addition of stringers and rings [6, 7]. As mentioned previously, the positioning of cutouts as geometric discontinuities creates a structure which is extremely practical. A literature search indicated very little work, either experimental or analytical, in the area of stiffened cylindrical shells with cutouts. Thus, the author has carried out such a study with the assistance of the STAGS program. The remaining portion of this paper will discuss the

- linear bifurcation solutions for both ring and ring-stringer stiffened cylindrical shells with particular interest given to convergence of results due to finite difference refinements.
- collapse nonlinear solutions for the above mentioned shell structures. Comparison has been made between linear and nonlinear solutions.
- comparison between smeared and discrete stiffener results.
- geometry and stiffener effect on buckling.
- buckling load increase due to stiffening in the area of the cutout.

LINEAR AND NONLINEAR RESULTS

The primary concern of this section is to establish, for the shell

geometries investigated, a finite difference mesh arrangement which can be used in collapse load solutions. Thus, one is looking for a grid system that reduces convergence difficulties and also handles any large displacement gradient which may arise in the nonlinear solution. In order to approach the optimum finite difference approximation economically, one should first do a great deal of parametric study using the simpler linear bifurcation theory.

Figure 1 shows the shell properties incorporated into the convergence and nonlinear investigations. One should notice the clamped boundary conditions assumed plus the rectangular shaped internal stringer. Since the loading conditions are taken to be axially symmetric, the analysis has been carried out over a one-eighth shell section imposing the prebuckling and buckling boundary conditions for a linear solution.

As previously mentioned, a collapse shell load value can only be confidently evaluated, using a numerical finite difference technique, if convergence characteristics are established. This is usually done through first considering linear bifurcation results. Figure 2 indicates P_{cr} values found for a shell with a 24" x 24" cutout using various nodal arrangements. One notices the increase in the number of nodes within a finite difference mesh arrangement. Figure 3 shows that, if a discrete stiffener approach is incorporated into the study, convergence becomes erratic; i.e., the buckling load is not monotonically increasing or decreasing with respect to the number of nodes. Yet, smeared theory results show a definite convergence trend from above. In both sets of results, a scatter of solutions amounts to no more than 3 percent. Consequently, it is possible to obtain good results, again

for the governing conditions, using approximately 600 nodal points spaced such that a circumferential mesh line is present at and between stringers and an axial mesh line is separated as far apart as the stringers spacing.

In order to further convince the reader that a detailed refinement of mesh size is unnecessary even with a 24" x 24" cutout, one may observe the next sequence of diagrams. Figures 4 through 8 present data representing stress flow and buckling modes in the area of the cutout. Discrete and smeared theory are evaluated making use of two different mesh refinements. It becomes obvious that not only do the smeared and discrete theories give close results, but a mesh arrangement of one line between stringers gives almost the same stress values as an arrangement with three mesh lines. This insensitivity is apparently due to the stiffening effect produced by the stringers.

The author believes that it is now possible to evaluate a collapse load for the structure considered using a mesh arrangement consisting of 602 node points with one mesh line at and between stringers. Figures 9 and 10 give values that are both within reason and satisfy good convergence characteristics. Figure 9 shows the closeness between collapse and bifurcation loads. The figure depicts a load displacement curve for that point displacing the greatest quantity using a nonlinear technique. From Figure 10, it may be observed that a collapse wave, along the bottom boundary, contains no large displacement gradients. Furthermore, it is interesting to note that the pre-bifurcation curve is much different than the collapse displacement. Yet, the buckling loads are relatively close. This is due primarily to the increased stiffness present in a linear analysis which produces a less sensitive moment effect.

The work discussed up to this point relates to stringer stiffened cylindrical shells. A like study has been carried out for a shell stiffened by both internal stringers and rings with a 27" x 24" cutout.

A smeared theory approach was only used in the convergence investigation for this particular skin configuration. Again, as Fig. 11 indicates, the smeared theory gives convergence from above. One obtains a critical load value, for 714 node points with mesh lines between stringers and at the ring locations, which is within 4 percent of the value obtained using 2262 nodes. Thus, mesh refinement does not appear to be necessary. Figures 12 and 13 present the collapse load and mechanism for the shell. There is a larger collapse load compared to the bifurcation value, but the difference amounts to only 11 percent. Furthermore, it is shown in Fig. 13 that the displacement collapse wave does not change drastically and therefore can be considered well behaved with at least five nodes per half wave. Thus, it appears the mesh arrangement is adequate.

STIFFENING AROUND CUTOUTS

A limited investigation has been carried out into discrete stiffener effect upon shell cutouts. This section discusses certain findings for such a study.

It is conceivable to use the STAGS program as a tool analogous to physical experimentation. As stated in the Introduction, most cutout stiffener problems are handled through a trial and error solution. A good illustration of this experimentation approach can be obtained in research performed by McDonnell Douglas [1]. In this work a thin stiffening frame was placed adjacent to a cutout within the

interior surface of a Thor Delta Interstage cylinder. The effects of a cutout and its reinforcement on buckling behavior were explored experimentally by physically varying the stiffener position to overcome any skin rippling. It is now possible to explore the same problem by incorporating STAGS into the solution without resorting to extensive experimentation.

Figure 14 indicates cutout stiffening results for the stringer stiffened shell geometry (27" x 24" cutout) discussed previously using the 602 node finite difference scheme shown in Fig. 2. Two types of stiffened arrangements have been studied. The first is a discrete rectangular frame (Area = 2.18 sq. in.) placed internally around the opening. A plot is shown for each frame position relating a ratio of stiffener weight to cutout weight removed against the critical load normalized to a shell with no openings. It can be observed that as the discrete frame is increased in volume, through a change in position, the critical buckling value approaches results close to those possible without any shell opening. An optimum frame position is possible which gives a higher buckling value compared to other positions (see position 4). The second cutout stiffener studied is developed by increasing the shell thickness along its internal surface. The cross section and a plot of the weight to critical load ratio can also be found in Fig. 14. Two stiffener widths have been evaluated producing points A and B in the plot. It is apparent that as the size of cross section increases the critical buckling ratio approaches the value for a shell with no cutout.

The reader can observe in Fig. 15 bifurcation comparisons for a ring and stringer stiffened shell with cutout reinforcements similar

to the stringer stiffened shell just discussed. It is shown that as the discrete frame volume increases with location, the bifurcation ratio P/P_o decreases. Yet, as the thickened reinforcement increases in volume, a bifurcation ratio almost equal to one occurs.

STRESS SURROUNDING THE STIFFENED CUTOUT

An attempt has been made to determine the overall effect due to cutout stiffening by investigating stress redistribution and eigenvector comparison at bifurcations. Figure 16 presents the stress field, at the interior stringer stiffened shell surface, surrounding a cutout in which a stiffening frame is positioned adjacent to the opening similar to Fig. 14. In order to compare values to non-stiffened cutouts, stress quantities have been normalized. The reader can observe that the stress values decrease in areas adjacent to the discrete stiffener. Yet, immediately above the frame one can find highly concentrated σ_x contours. Figure 17 indicates, for the same frame positioning shown in Fig. 16, the complete reorientation of bifurcation waves along the cutout edge as well as other frame axial coordinates. Points of maximum buckling wave amplitudes are depicted for specific angular measurements. One can appreciate that not only are the half wave locations different between shells without cutout frame stiffeners, but the circumferential wave number is also affected. Figure 18 is a presentation of the same stress and buckling wave effect discussed in the above two mentioned figures, but in this case cutout stiffening is created by a thickened shell skin. Results indicate a similar total effect.

EFFECT OF SHELL AND STIFFENER GEOMETRY

Investigators of problems related to cutouts in smooth surface cylindrical shells [8] have determined a generalized cutout parameter.

This parameter is the $a/(Rt)^{\frac{1}{2}}$ ratio in which 2a equals the cutout width; R and t are the shell's radius and thickness respectively. The writer tried to produce a similar parameter for cutouts in stiffened shells. This section described some of the work performed.

Figure 19 shows a plot of cutout parameters used in reference [8] for the present problems. It becomes obvious that a parameter similar to smooth surfaced shells was not appropriate for stiffened shells since a common curve is not obtained. The cutout effect turns out to be very different compared to smooth shells because of the stiffening produced in cutout regions. Therefore, a study of possible stiffener geometry effects on cutouts was pursued. Figures 20 and 21 indicate a greater shell sensitivity to variations in a stringer's axial rigidity for given cutout sizes as compared to a stringer's flexural stiffness. Consequently, the author explored various axial stiffness parameter combinations by including or excluding the shells axial rigidity. The success in obtaining an ideal function can be found in Figs. 22 to 24. Observation reveals that simple geometric stiffener area is not enough to establish a basic parameter. Yet, one may note an important property coming from this particular set of figures. It can be stated that nonlinear shell effects become apparent using small stiffener area; e.g., 0.05 sq. in., since the bifurcation curve reaches a minimum and increases for an increase in $a/(Rt)^{\frac{1}{2}}$ ratios. This has also been observed in reference [8]. A reason for this inconsistency may be attributed to the elimination of moment effects in linear bifurcation theory and thus, as cutout size increases a tension field occurs using linear analysis which would normally be overcome if nonlinear relationships were incorporated.

An additional study was pursued, this time in relation to the stiffener and shell flexural rigidity. It was previously stated that a cutout is less sensitive to a flexural parameter. Results verified this conclusion as shown in Figs. 25 and 26.

As a final investigation phase, the author attempted to combine axial and flexural rigidity. Figure 27 indicates some success for reasonable shell thicknesses.

CONCLUSIONS

It is now possible to make the following conclusions:

1). The STAGS program has been used in studying buckling characteristics for a stringer stiffened, in addition to a ring and stringer stiffened, shells. The bifurcation load is within 11 percent of the collapse force for each configuration, and thus it is possible to study buckling loads using linear analysis for configurations similar to those investigated herein.

2). Previously, cutout reinforcement was determined by a trial and error experimental approach. STAGS makes it possible to investigate this problem and determine the most effective reinforcement position.

and 3). The study reported upon reveals that the parameter $a/(Rt)^{\frac{1}{2}}$ used in isotropic shells considering cutouts is not appropriate for stiffened shells.

REFERENCES

R. F. Snell, Experimental Evaluation of the Effects of Cutouts on the Stress State and Buckling Stability of the Isogrid Structures of the Thor Delta Interstage and Fairing, MDC Report G2873, April, 1972.

(2) D. Bushnell, B. O. Almroth and F. Brogan, Finite Difference Energy Method for Nonlinear Shell Analysis, Computers and Structures, Vol. 1, pp. 361-387.

(3) F. Brogan and B. O. Almroth, Buckling of Cylinders with Cutouts, AIAA J., Vol. 8, No. 2, Feb. 1970, pp. 236-241.

(4) B. O. Almroth and A.M.C. Holmes, Buckling of Shells with Cutouts, Experiment and Analysis, Int. J. Solids and Structures, Vol. 8, pp. 1057-1071, 1972.

(5) B. O. Almroth and F. A. Brogan, Bifurcation Buckling as an Approximation of the Collapse Load for General Shells, AIAA J. Vol. 10, No. 4, April 1972, pp. 463-467.

(6) J. Singer, Buckling of Integrally Stiffened Cylindrical Shells - A Review of Experiment and Theory presented at Van Der Neut Symposium, 1972.

(7) D. L. Block, Influence of Discrete Ring Stiffeners and Prebuckling Deformations on The Buckling of Eccentrically Stiffened Orthotropic Cylinders, NASA TN D-4283, January 1968.

(8) J. H. Starnes, The Effect of a Circular Hole on the Buckling of Cylindrical Shells, Ph.D. thesis, California Inst. of Tech., 1970.

FIGURE CAPTIONS

Fig. 1 Shell Geometric Properties

Fig. 2 Mesh Arrangement

Fig. 3 Number of Nodes vs. P_{cr} (Stringer Stiffened)

Fig. 4 σ_x Along x = 29 in. Mesh Line

Fig. 5 σ_x Along x = 33.5 in. Mesh Line

Fig. 6 Comparing Various Mesh Arrangements for N_{xy}

Fig. 7 N_{xy} Near Cutout

Fig. 8 Eigenvectors

Fig. 9 N_x vs w (Stringer Stiffened)

Fig. 10 Displacement at x = 47 inches

Fig. 11 Number of Nodes vs. P_{cr} (Ring and Stringer Stiffened)

Fig. 12 N_x vs. w (Ring and Stringer Stiffened)

Fig. 13 Displacement at Collapse Along x = 47 inches

Fig. 14 Cutout Weight Ratio (Stringer Stiffened)

Fig. 15 Cutout Weight Ratio (Ring and Stringer Stiffened)

Fig. 16 σ_x at Bifurcation With Discrete Stiffener at Cutout

Fig. 17 Effect on Bifurcation Wave Due to Cutout Stiffeners

Fig. 18 Bifurcation Wave and Stresses for Thickened Skin

Fig. 19 Linear Buckling for Cylindrical Stiffened Shell

Fig. 20 Effect of Stringer Area on P_{cr}

Fig. 21 Effect of Stringer Inertia on P_{cr}

Fig. 22 Effect of Stringer Area and Opening on P_{cr}

Fig. 23 Effect of Stringer and Shell Extensional Area on P_{cr} (A_1 = 0.28 sq. in.)

Fig. 24 Effect of Stringer and Shell Extensional Area on P_{cr} (A_1 = 0.08 sq. in.)

Fig. 25 Effect of Stringer's Moment of Inertia on P_{cr} (A_1 = 0.08 sq. in.)

Fig. 26 Effect of Shell and Stringer's Moment of Inertia on P_{cr} (A_1 = 0.08 sq. in.)

Fig. 27 Effect of Combined Parameters on P_{cr}

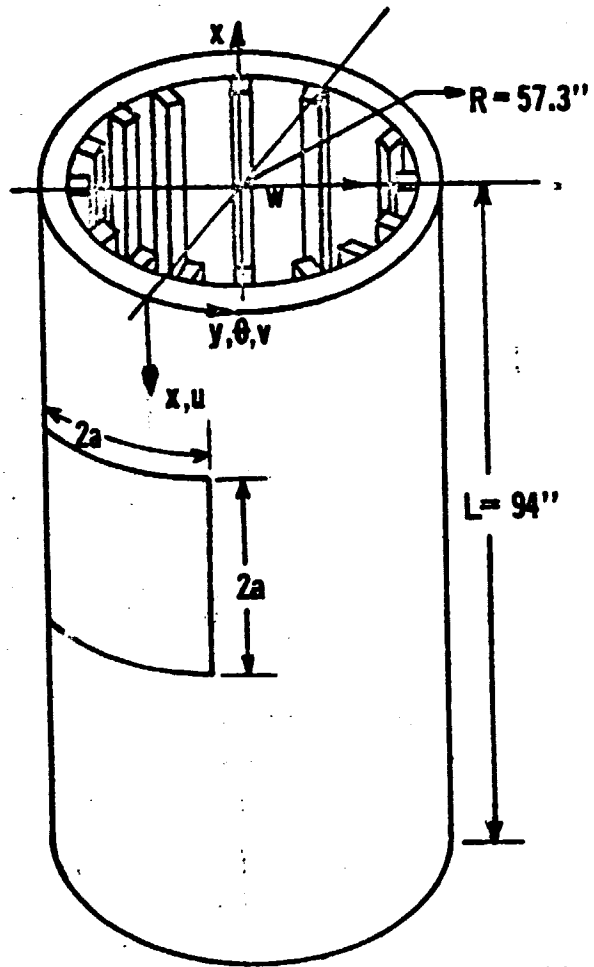

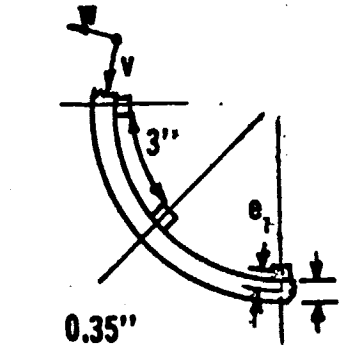

A_1 = area of stringer

$I_y = 0.01493$ in.^{4}

$GJ = 30302^{**}$ in.^{2}

$E = 10{,}000$ ksi

A_2 = area of ring

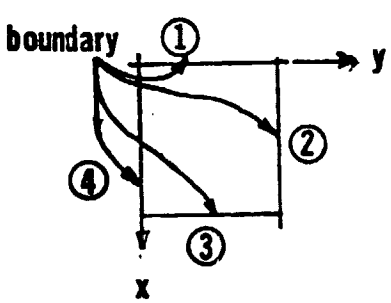

Clamped

pre-buckling		buckling
② ; $v = \beta = 0$	⟷	
③ ; $u = \beta = 0$	⟷	same
④ ; $v = \beta = 0$	⟷	
① ; $w = v = \beta = 0$, $u = 0.09$ in.		$w = v = u = \beta = 0$

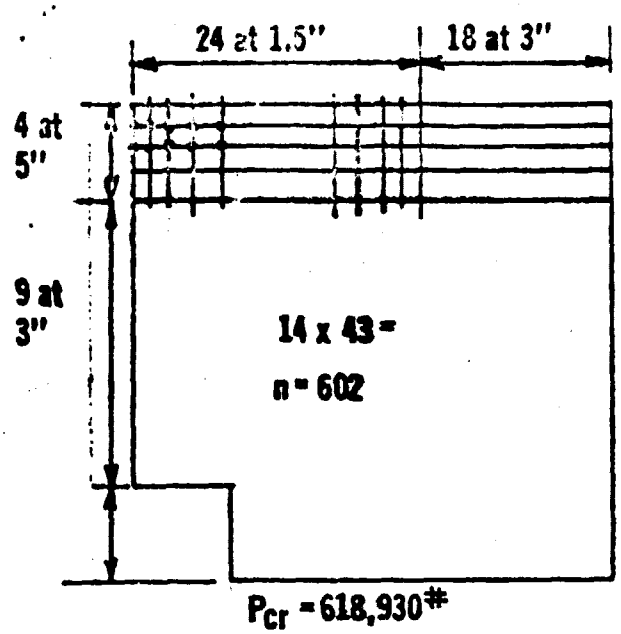

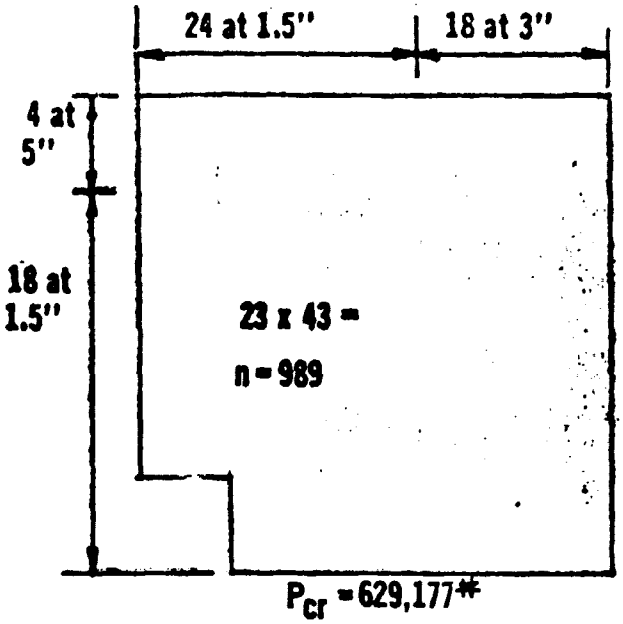

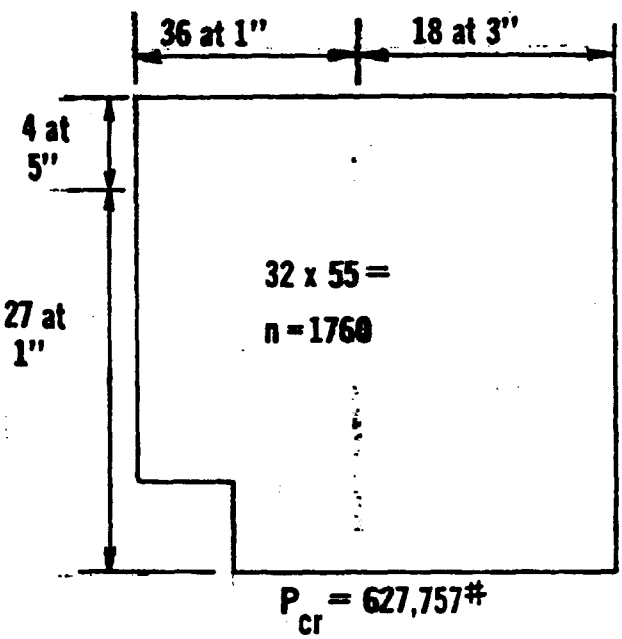

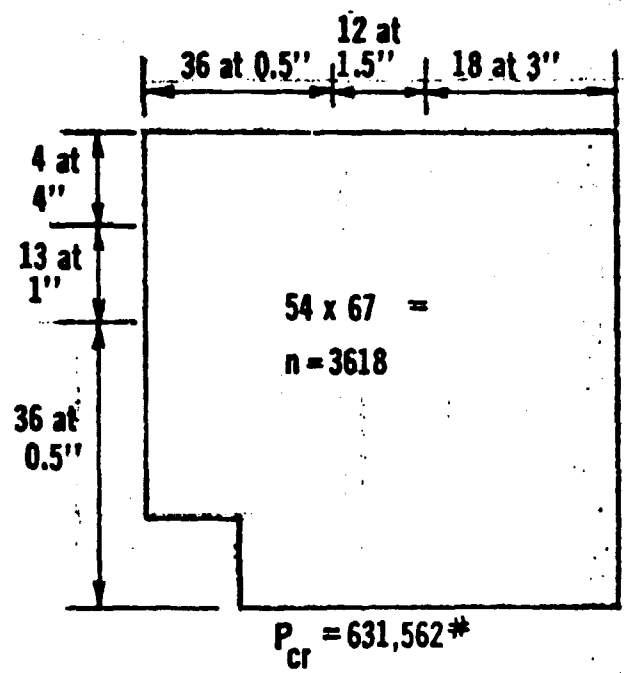

n number of modes

R = 57.3" L = 94" A_1 = 0.28 " b_1 = 3"

Cutout = 24" x 24" Discrete Stringer Approach Used

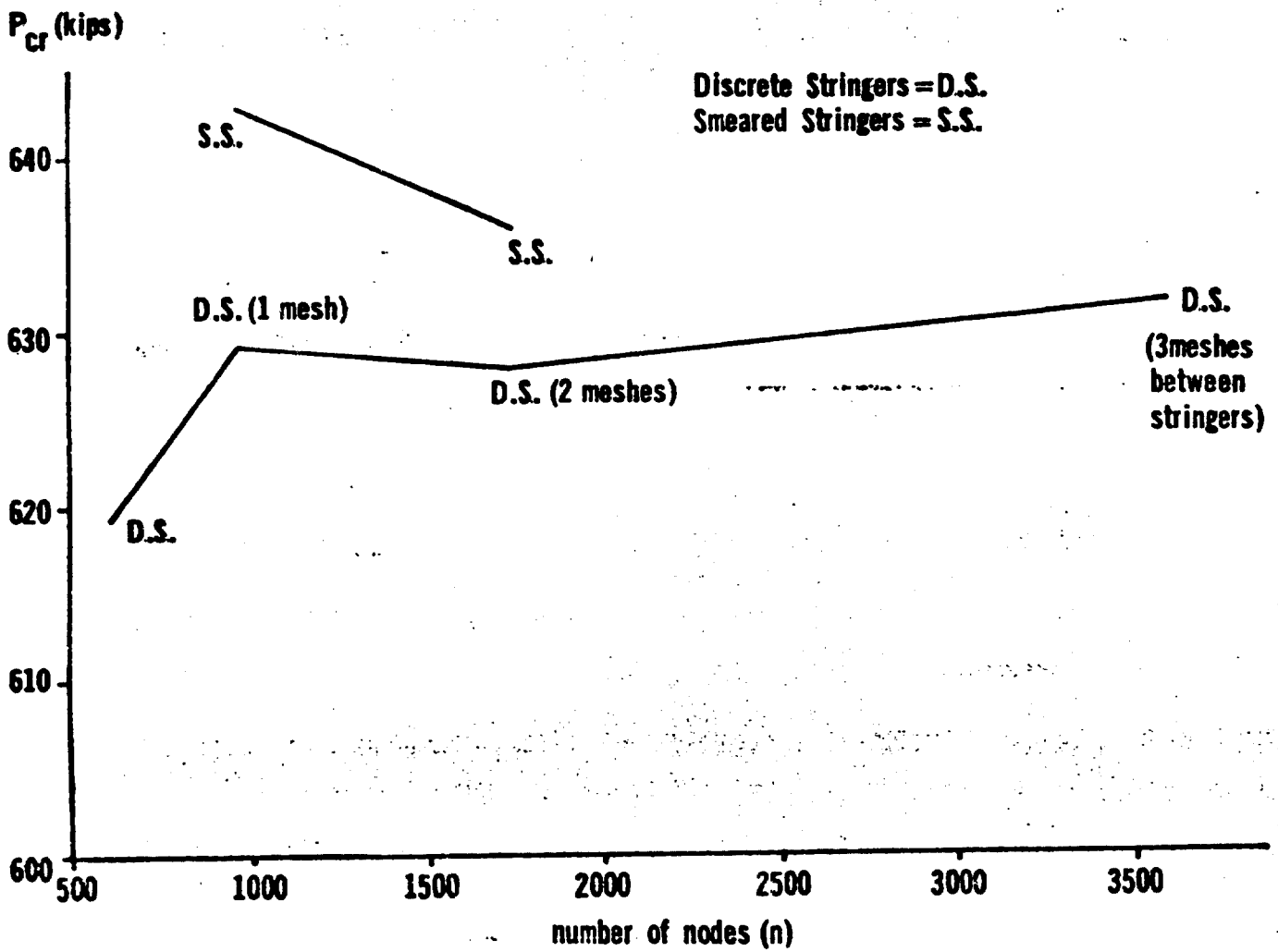

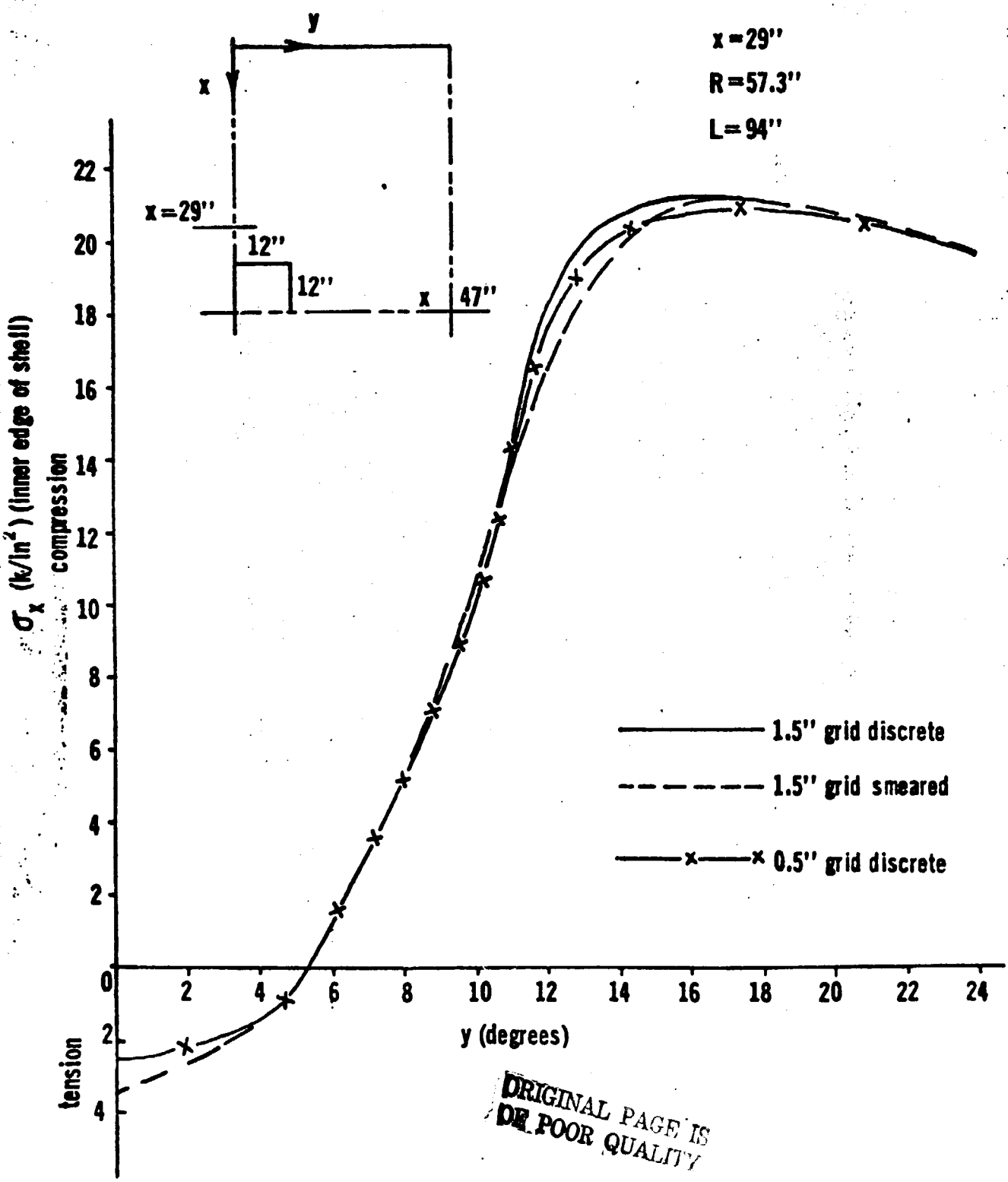

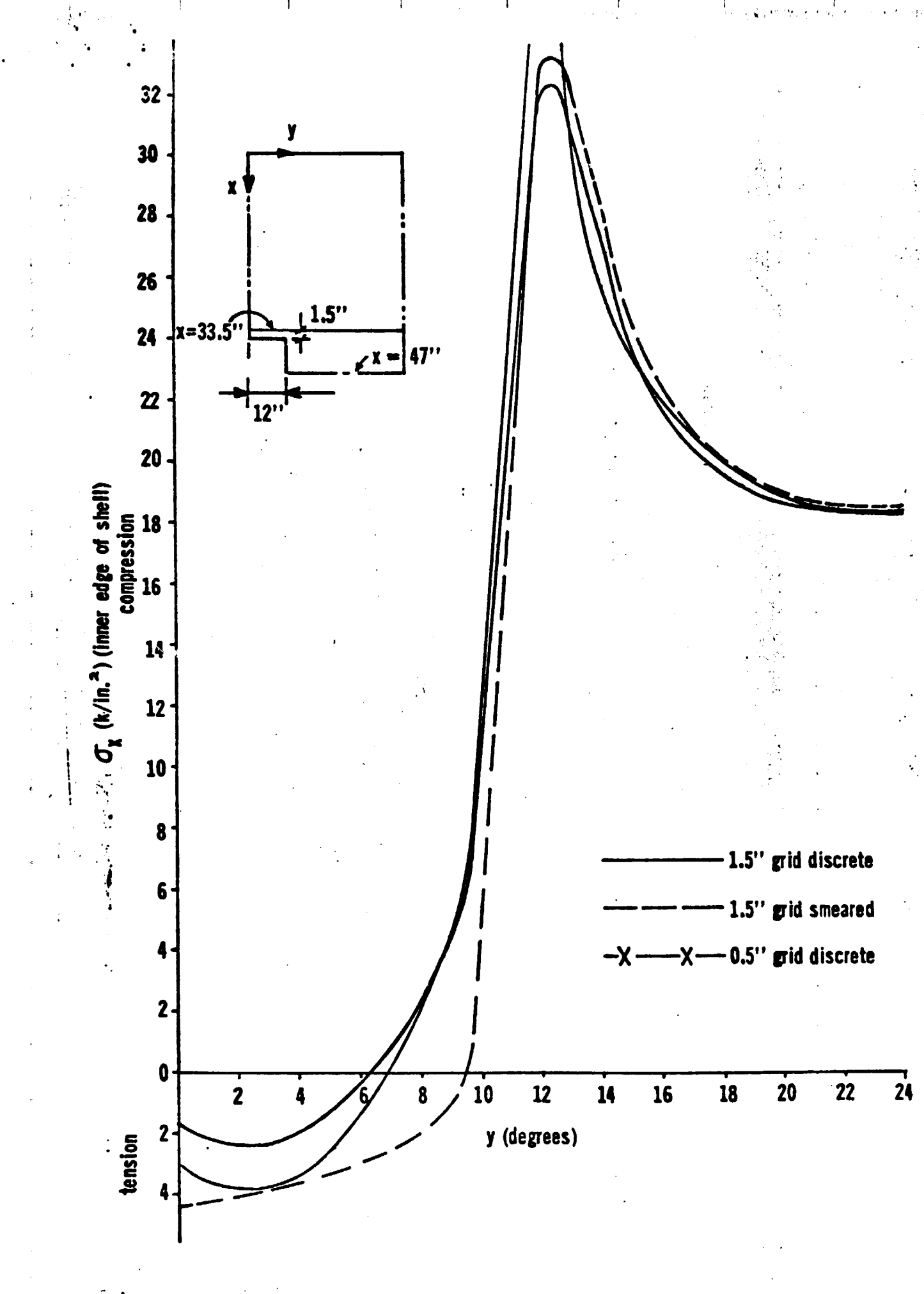
y
x
x=33.5"
1.5"
x = 47"
12"
σ_x (k/in.^{2}) (inner edge of shell)
compression
tension
y (degrees)
1.5" grid discrete
1.5" grid smeared
0.5" grid discrete

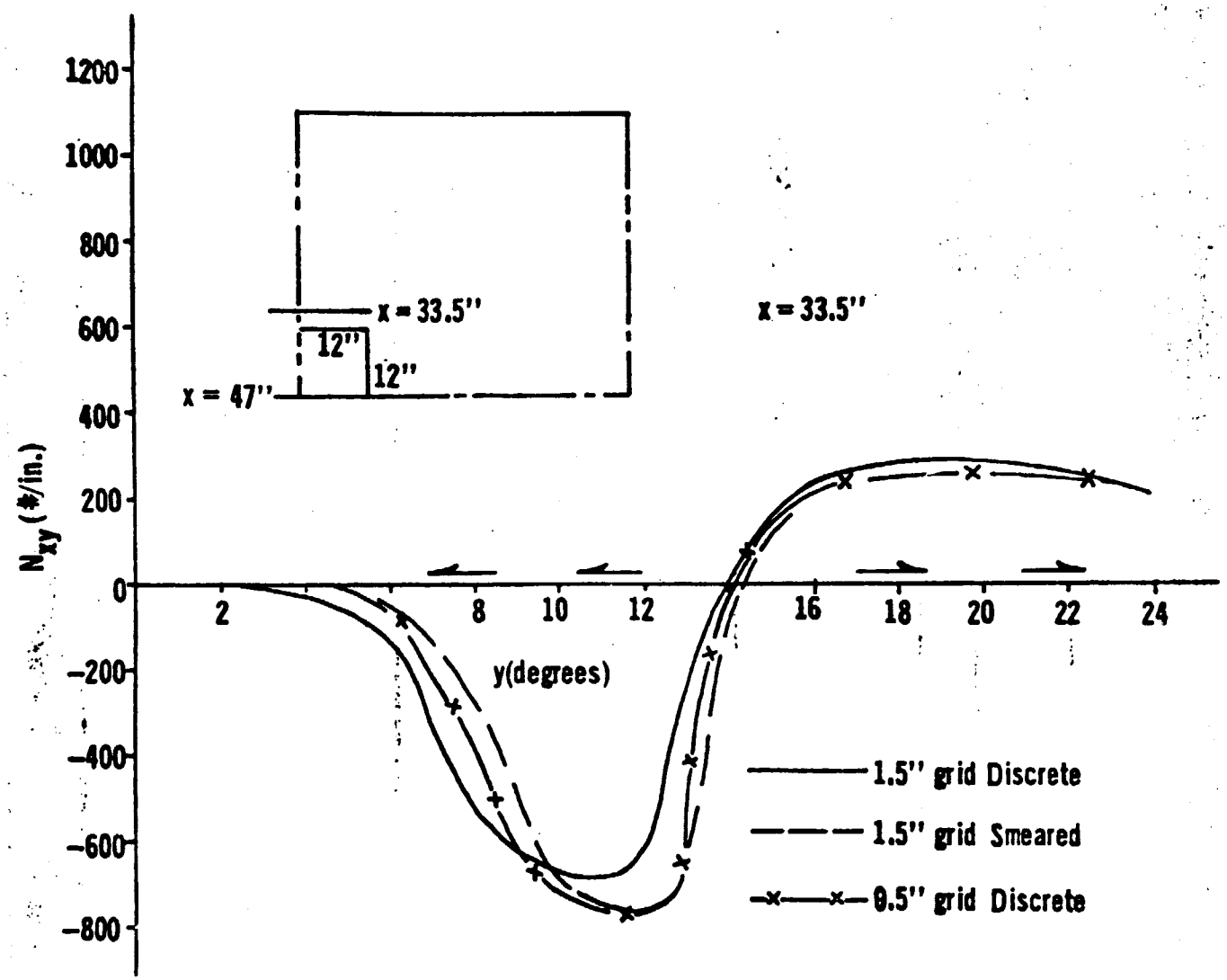

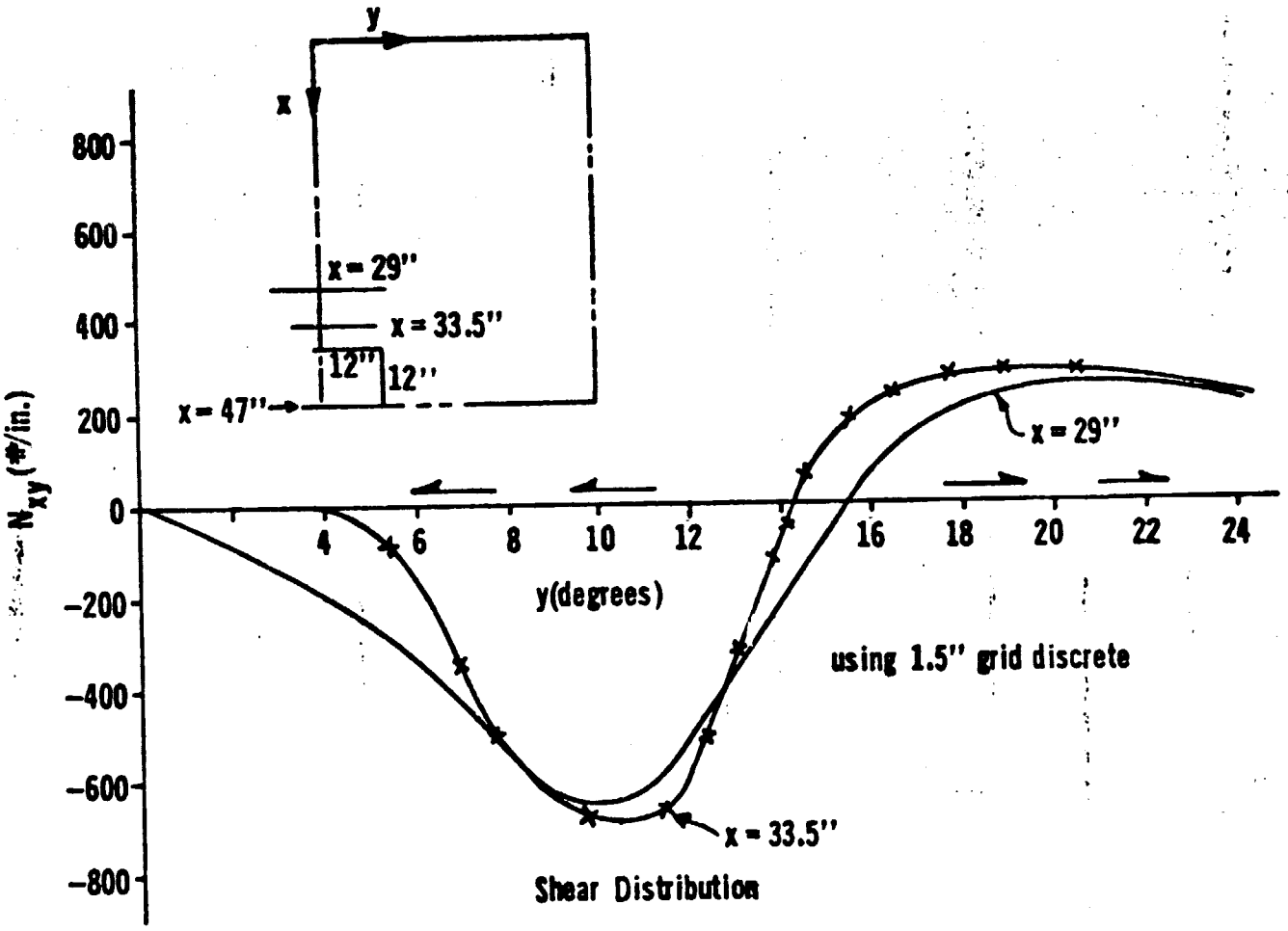

Shear Distribution

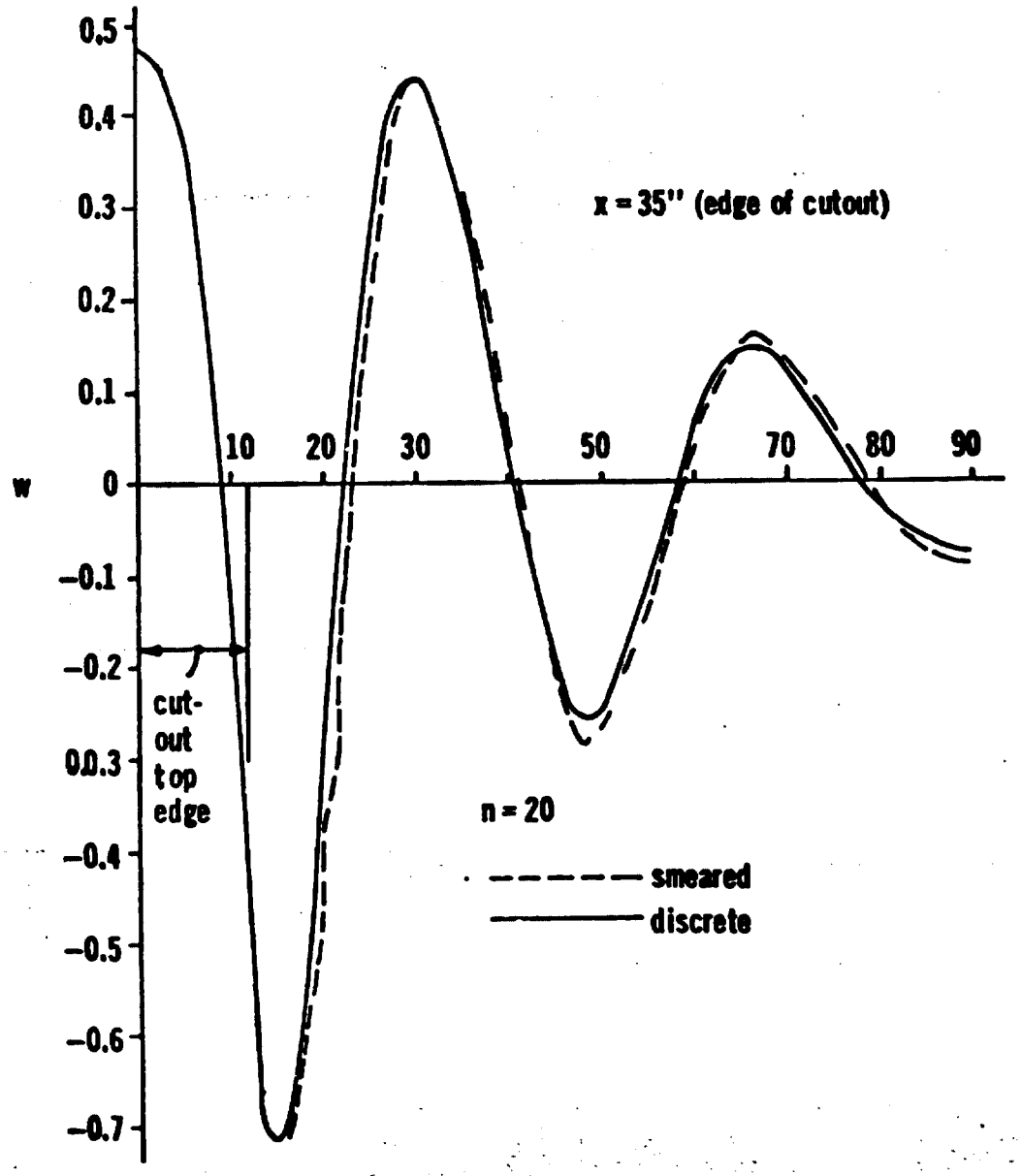

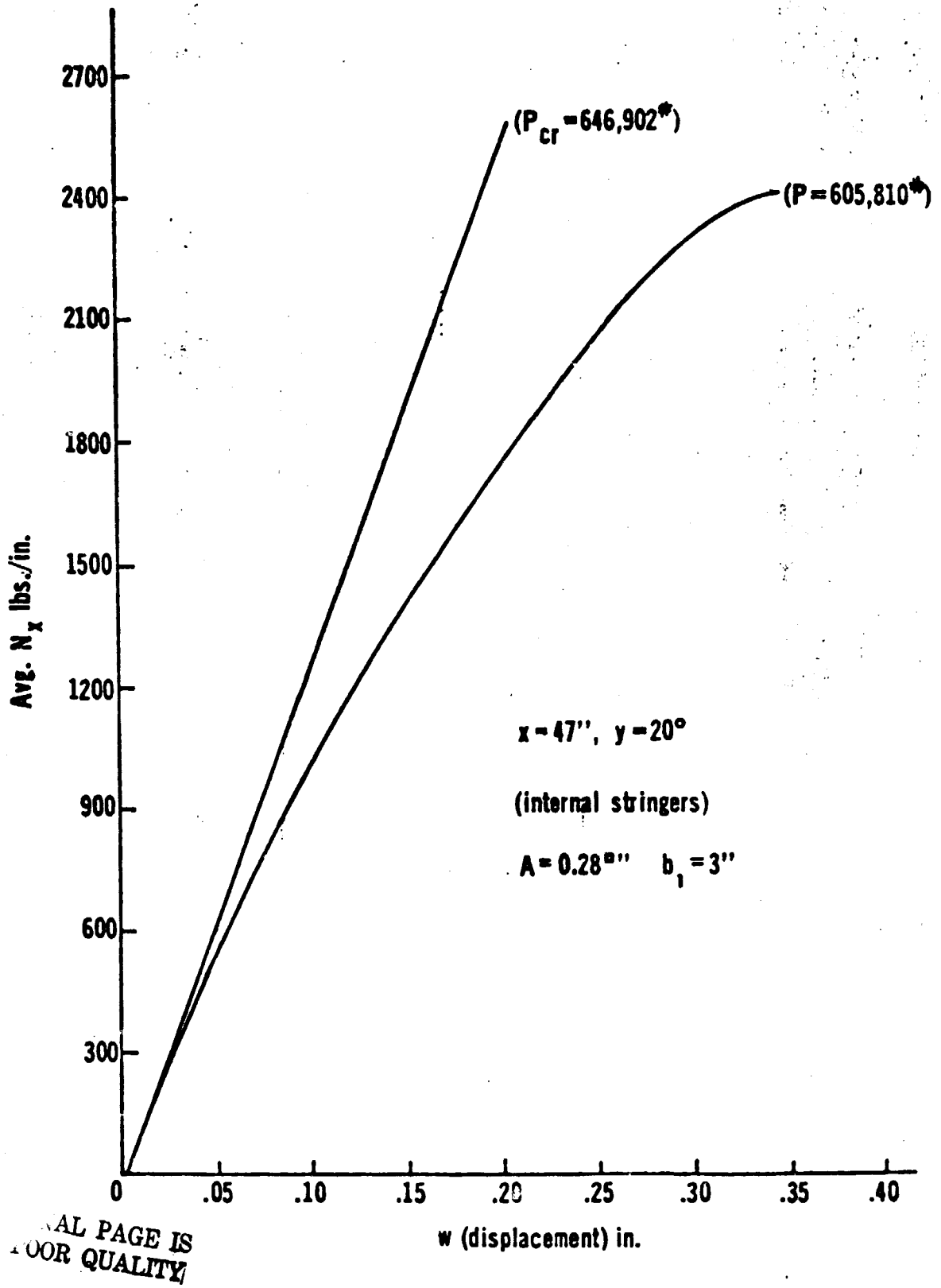

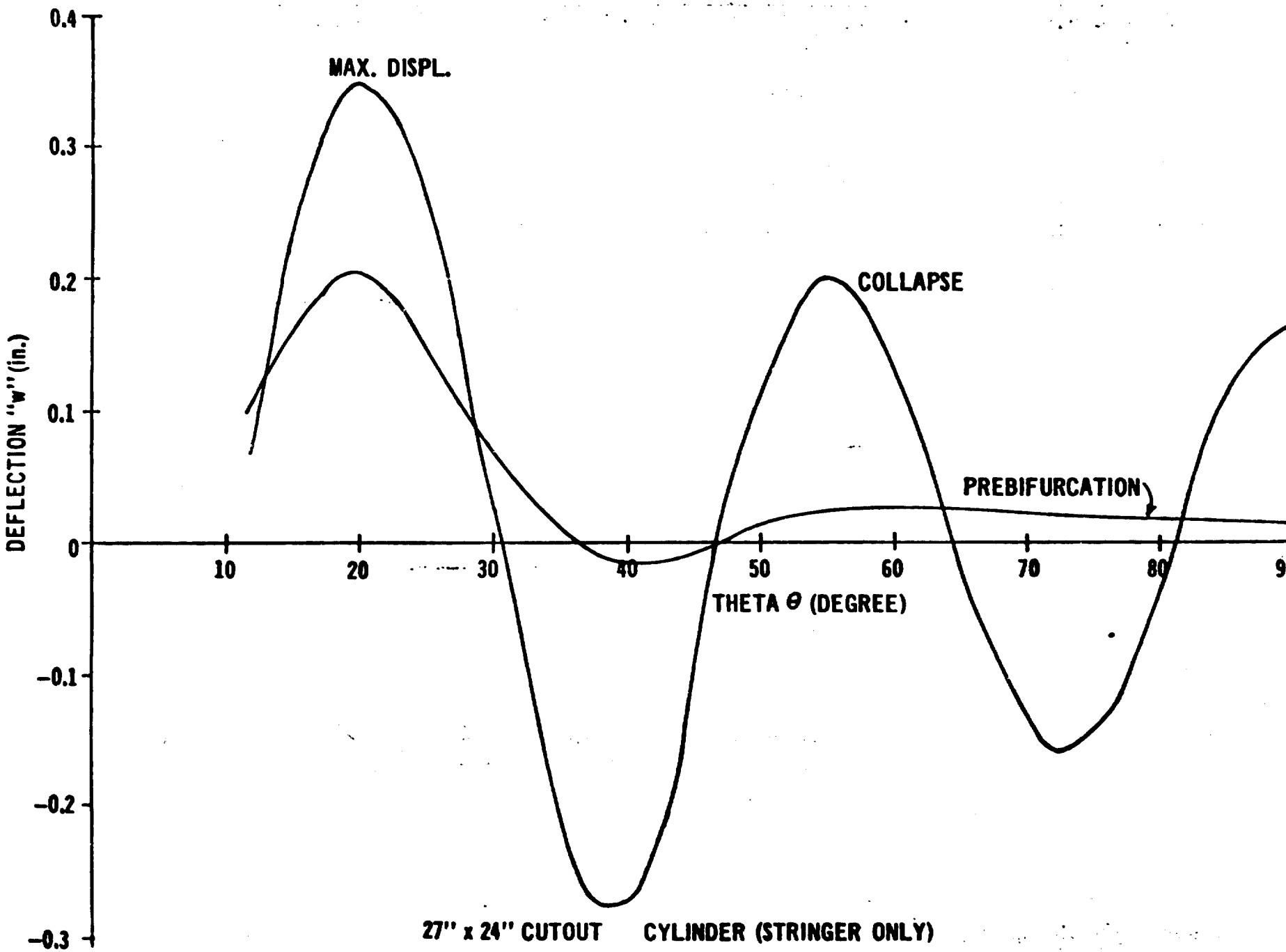
0.4
0.3
0.2
0.1
0
-0.1
-0.2
-0.3
DEFLECTION "w" (in.)
MAX. DISPL.
COLLAPSE
PREBIFURCATION
10
20
30
40
50
60
70
80
90
THETA θ (DEGREE)
27" x 24" CUTOUT CYLINDER (STRINGER ONLY)

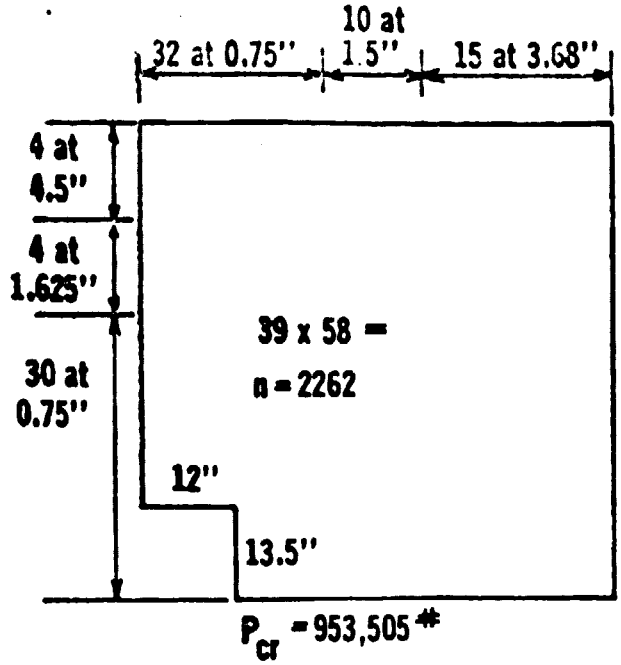

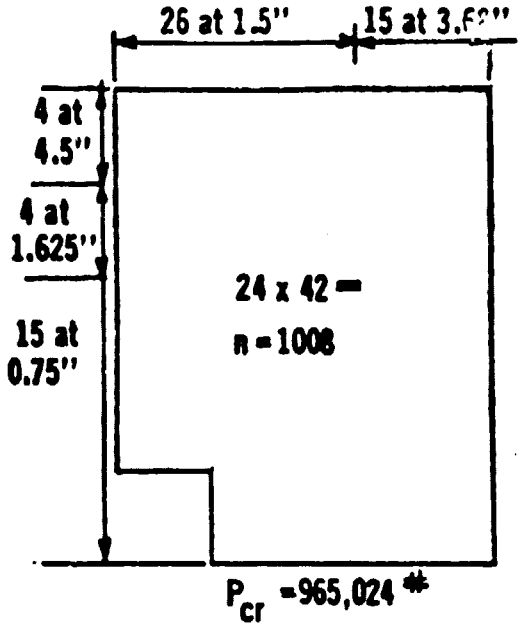

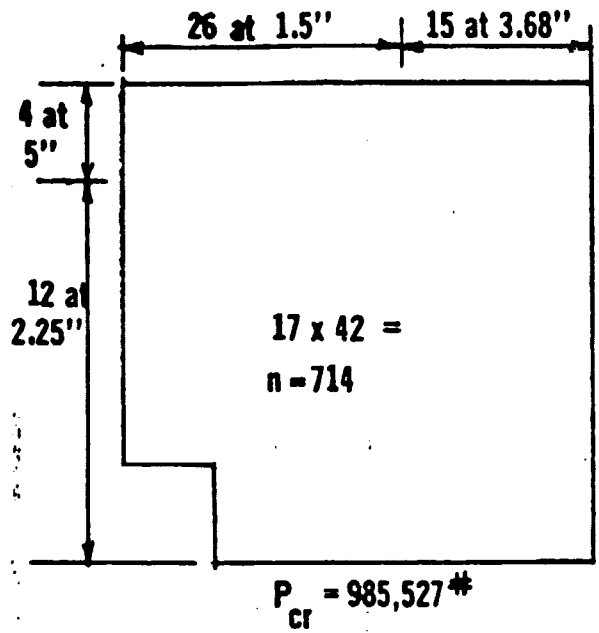

n = number of nodes
R = 60" L = 94
A_1 = 0.28 " b_1 = 3"
A_2 = 0.079 " b_2 = 4.5"
cutout 27" x 24"
smeared approach
Ring–Stringer

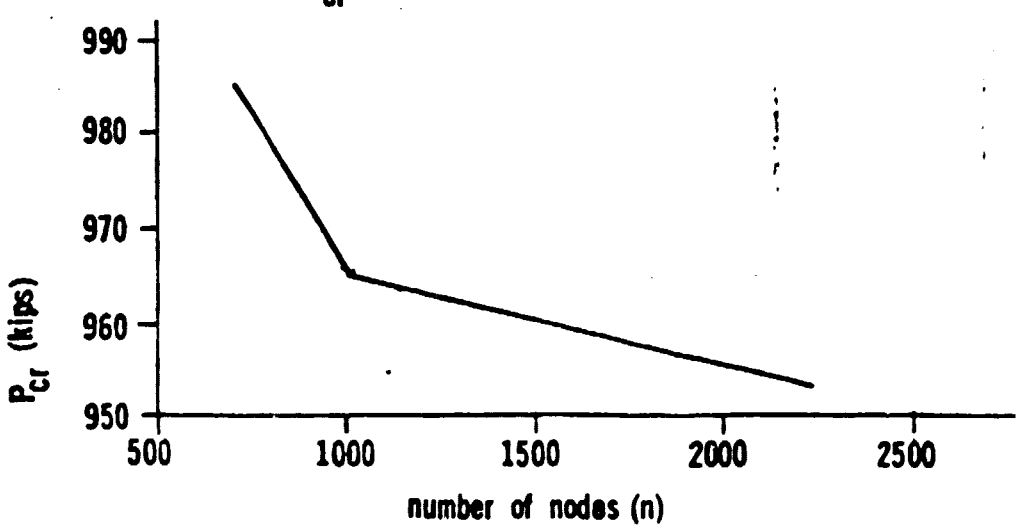

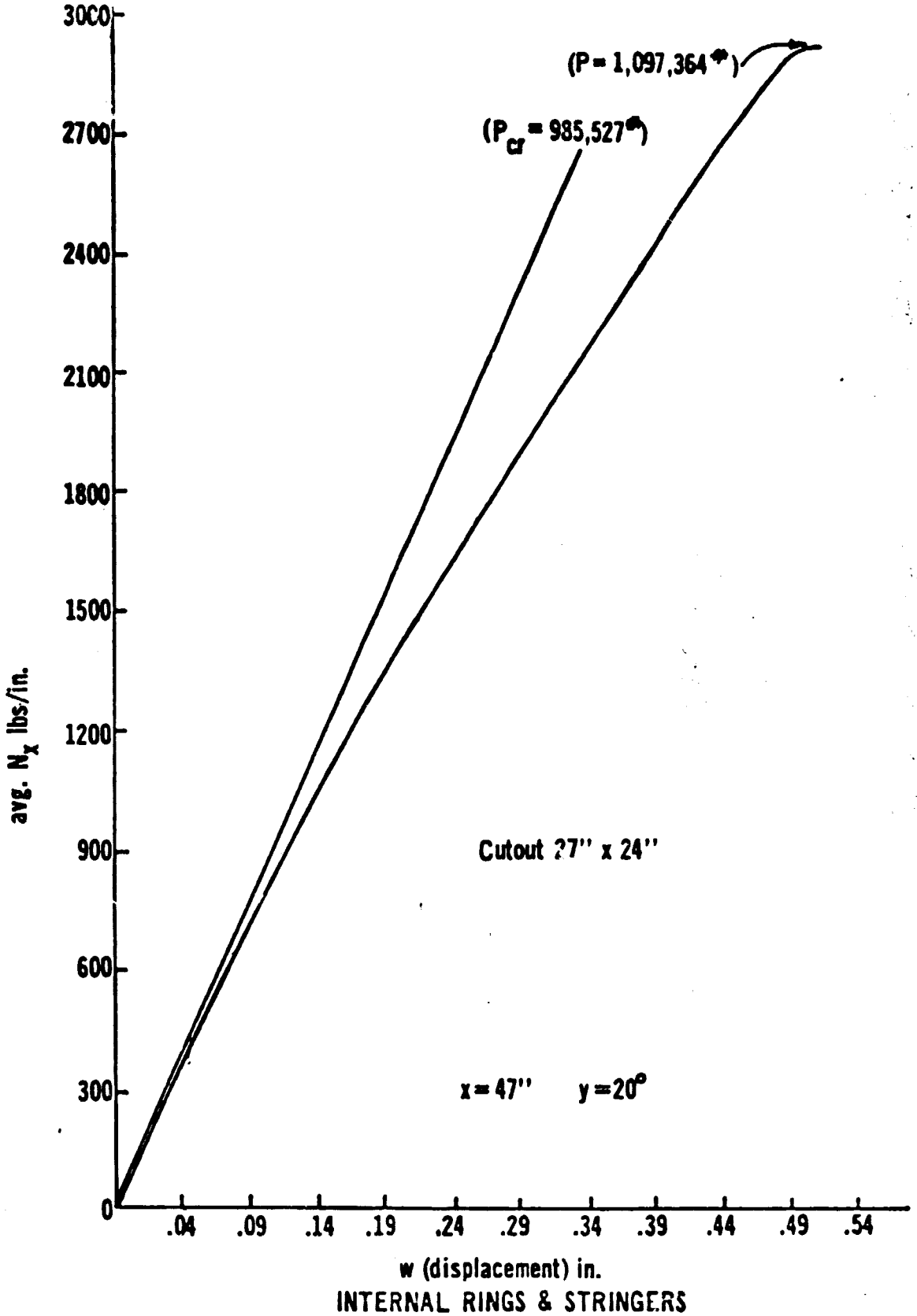
3000
2700
2400
2100
1800
1500
1200
900
600
300
0
avg. N_x lbs/in.
(P = 1,097,364 #)
(P_{cr} = 985,527 #)
Cutout 27" x 24"
x = 47"
y = 20°
.04
.09
.14
.19
.24
.29
.34
.39
.44
.49
.54
w (displacement) in.
INTERNAL RINGS & STRINGERS

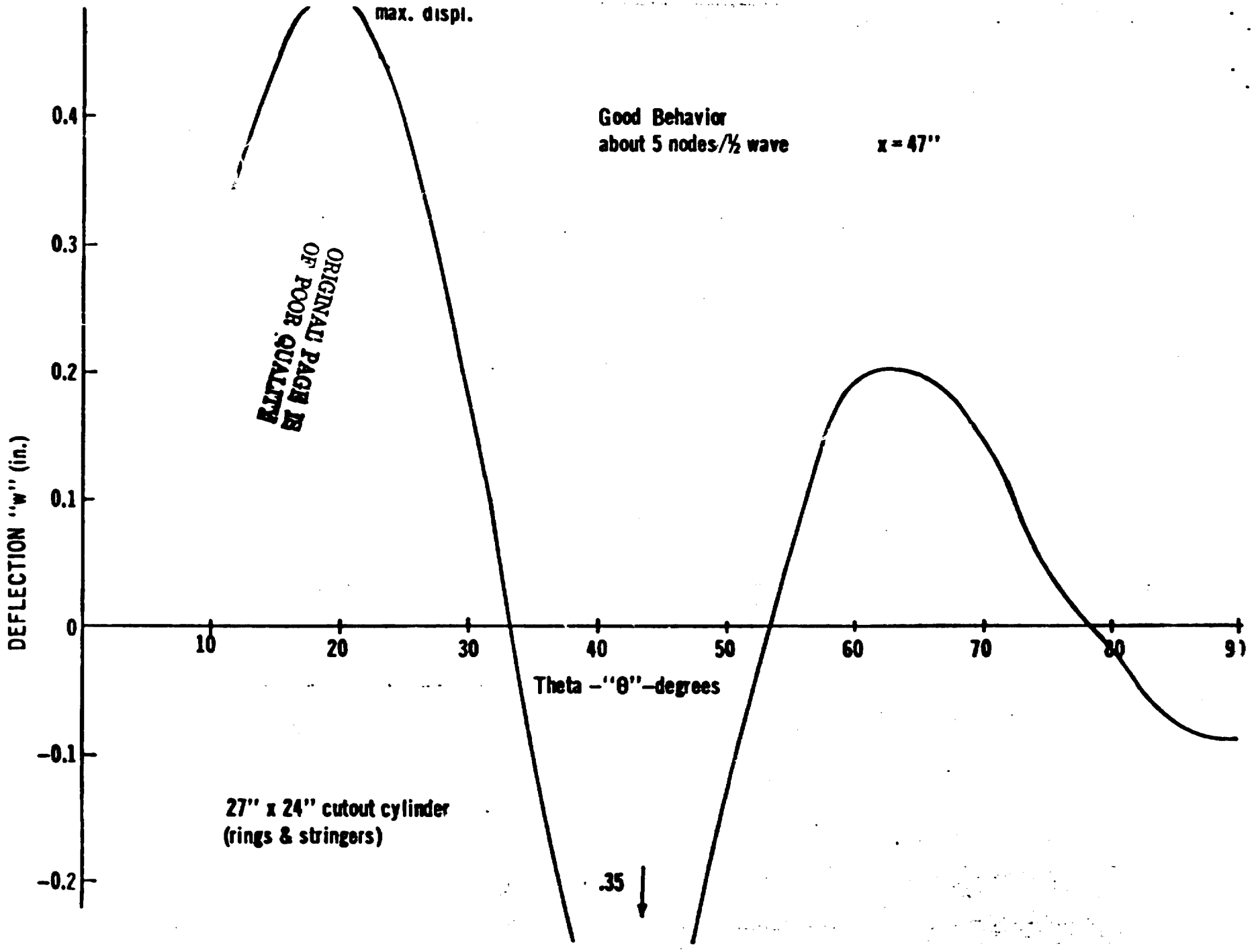
max. displ.
Good Behavior
about 5 nodes/½ wave
x = 47"
ORIGINAL PAGE IS
OF POOR QUALITY
DEFLECTION "w" (in.)
0.4
0.3
0.2
0.1
0
-0.1
-0.2
10
20
30
40
50
60
70
80
90
Theta –"θ"–degrees
27" x 24" cutout cylinder
(rings & stringers)
.35

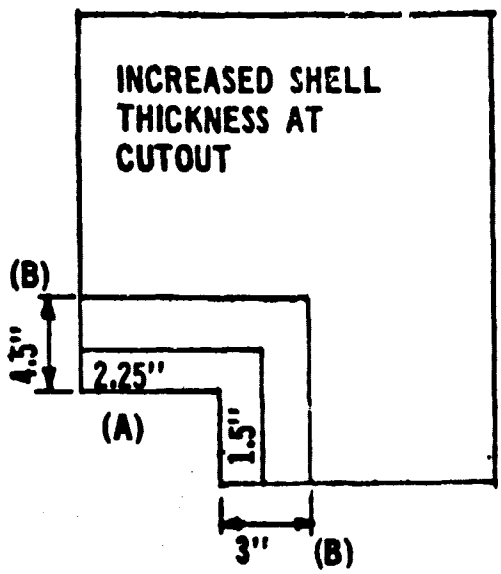

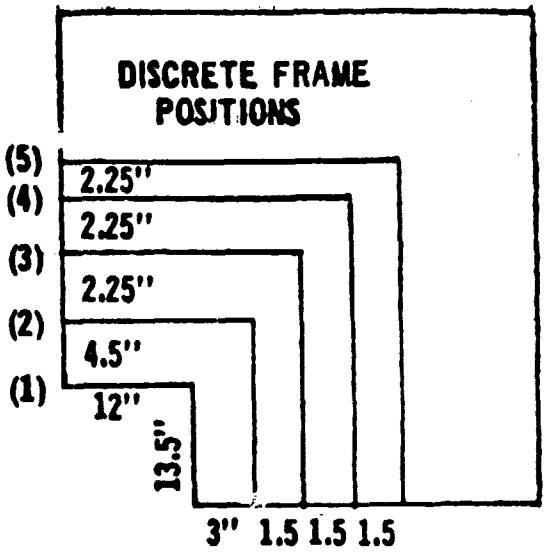

27"x24" CUTOUT

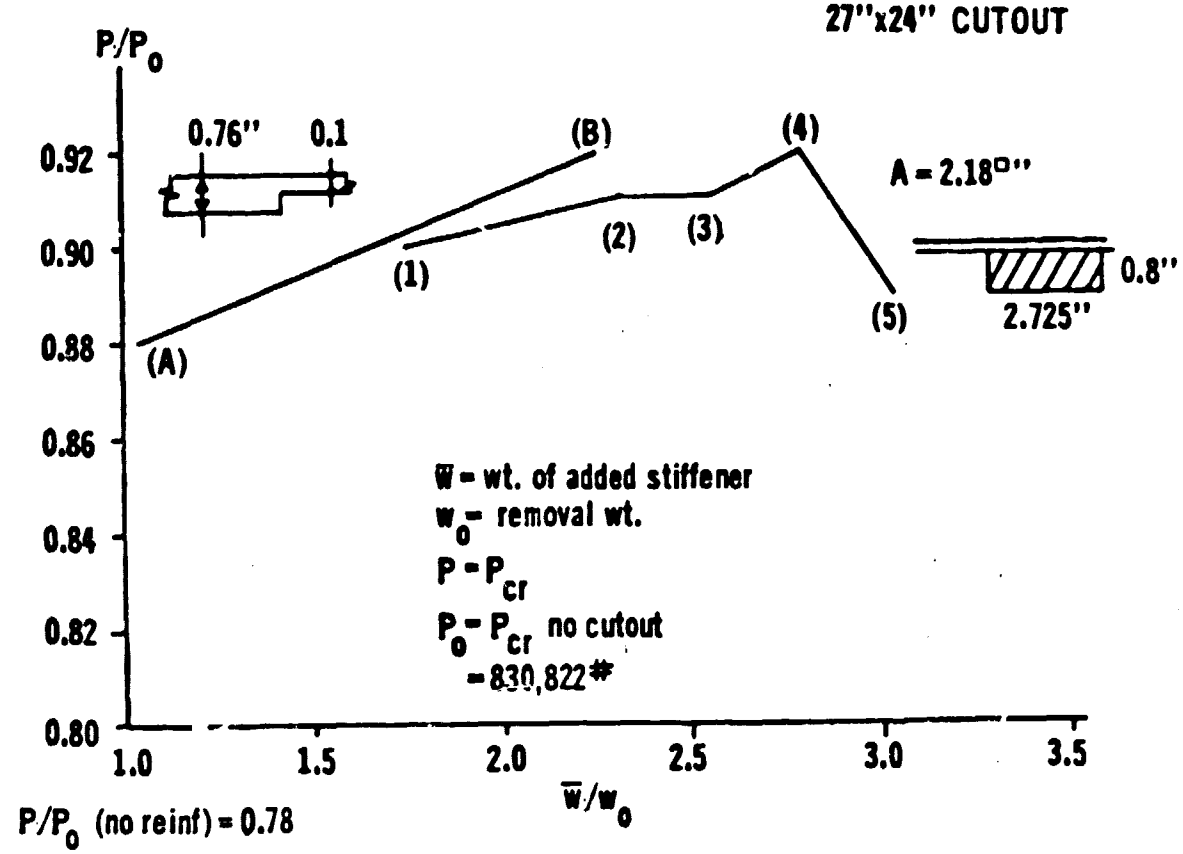

P/P_0 (no reinf) = 0.78

(Stringer Stiffened Cylindrical Shell)

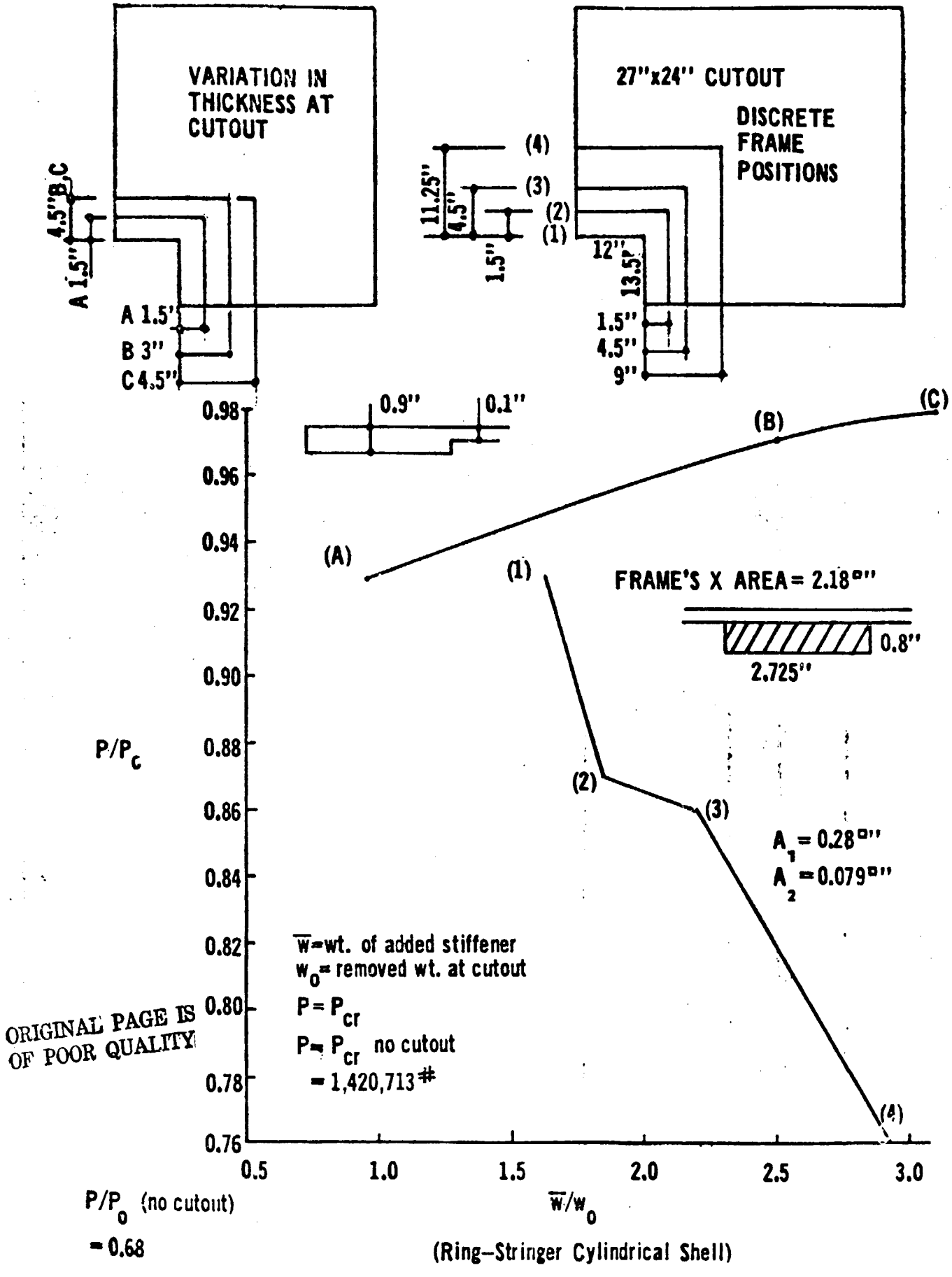

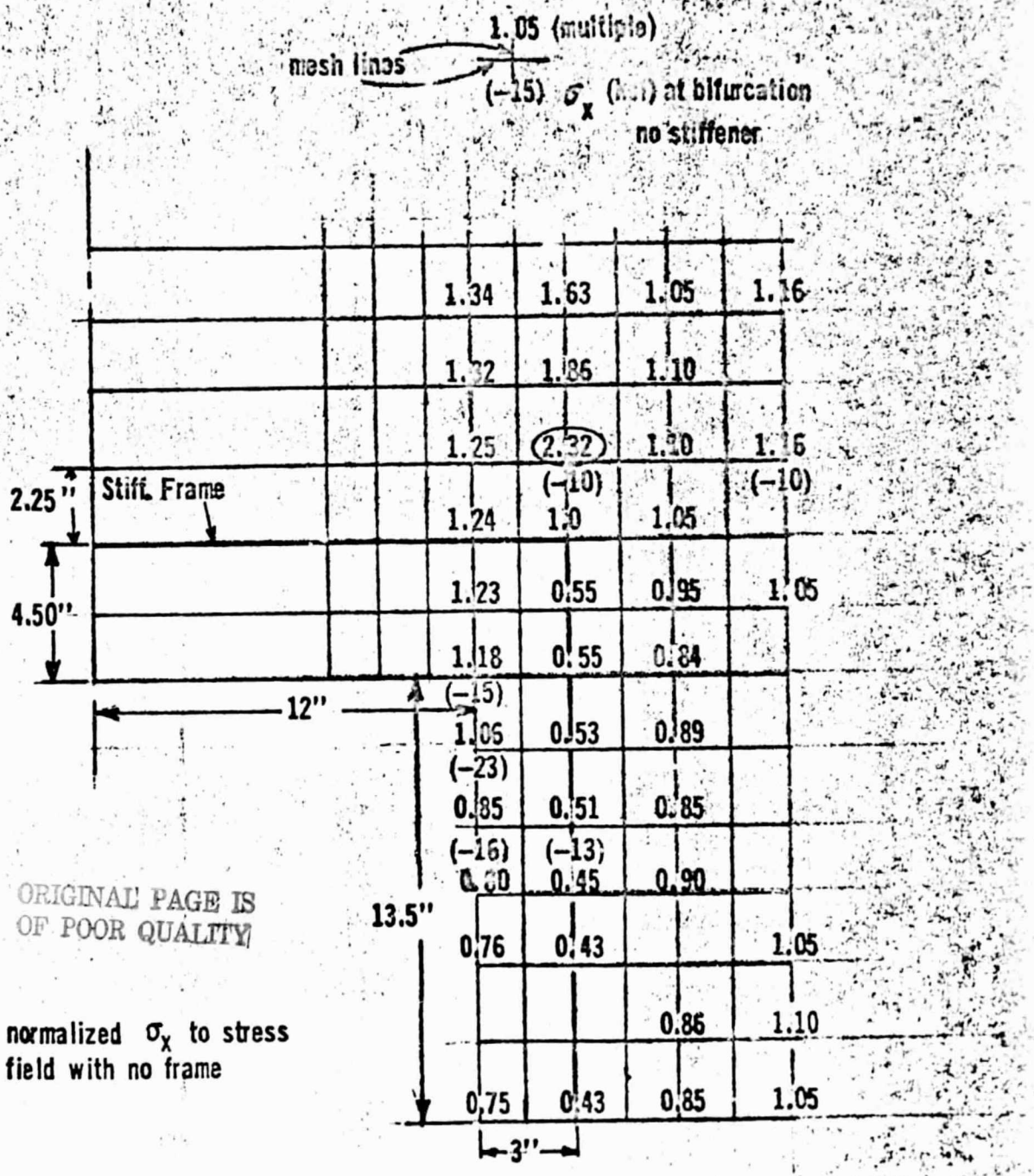

normalized σ_x to stress field with no frame

σ_x at Bifurcation (inner edge of shell) (stringer stiffened cyl. shell)

n = circumferential full value

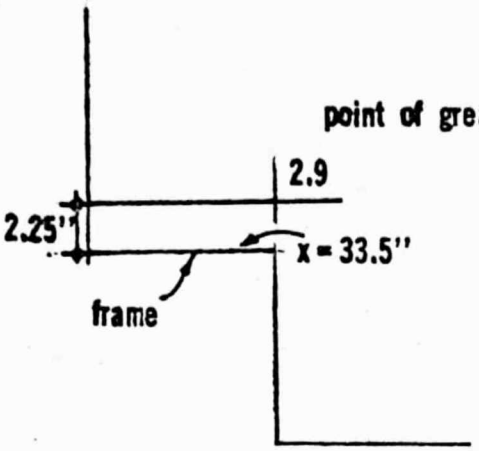

max. ampl. at x = 33.5"
frame 0°, 24°, 41°, 58°, 72° n = 10
no frame 0°, 14°, 30°, 48°, 62°, 76° n = 12

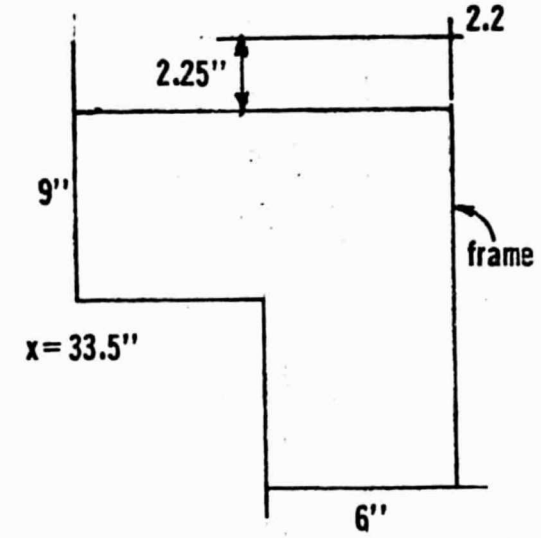

max. ampl. at x = 33.5"
frame 0°, 17°, 29°, 44°, 58°, 76° n = 12
no frame 0°, 14°, 30°, 48°, 62°, 76° n = 12

max. ampl. at x = 24.5" (frame)
frame 19°, 27°, 44°, 58°, 76° n = 10
no frame 0°, 16°, 30°, 48°, 62°, 76° n = 12

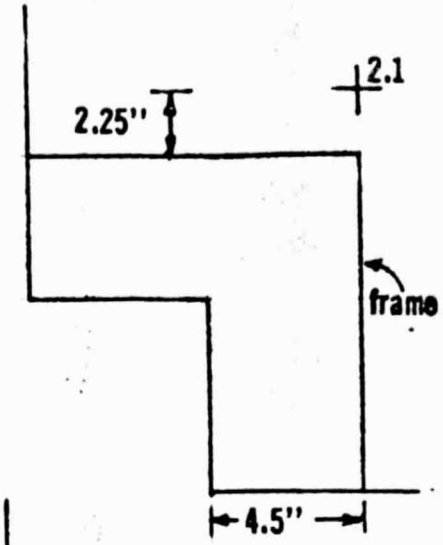

max. ampl. at x = 33.5"
frame 16°, 27°, 44°, 58°, 72°
n = 10
no frame 0°, 14°, 30°, 48°, 62°, 76°
n = 12

max. ampl. x 26.75"
frame 14°, 26°, 44°, 58°, 72°
n = 10
no frame 0°, 16°, 30°, 48°, 62°, 76°
n = 12

Note: 2.2 (multiple of stress at point with no frame)

ampl. = amplitude

(stringer stiffened cylindrical shell)

Fig. 1

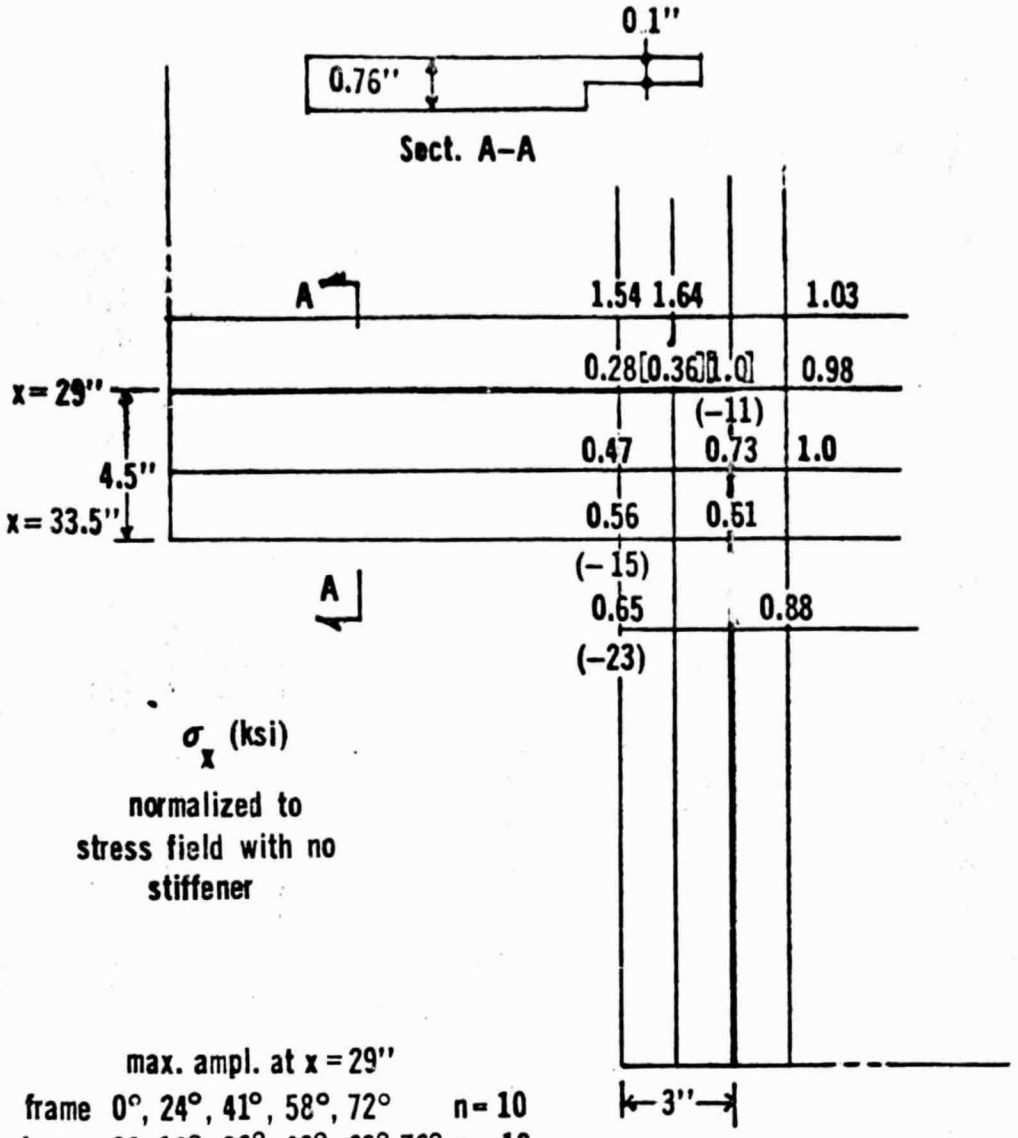

σ_x (ksi)

normalized to stress field with no stiffener

max. ampl. at x = 29"

frame	0°, 24°, 41°, 58°, 72°	n = 10
no frame	0°, 14°, 30°, 48°, 62° 76°	n = 12

max. ampl. at x = 33.5"

frame	0°, 24°, 41°, 58°, 72°	n = 10
no frame	0°, 14°, 30°, 48°, 62°, 76°	n = 12

ampl. = amplitude

n = full buckle wave

(Stringer Stiffened Cylindrical Shell)

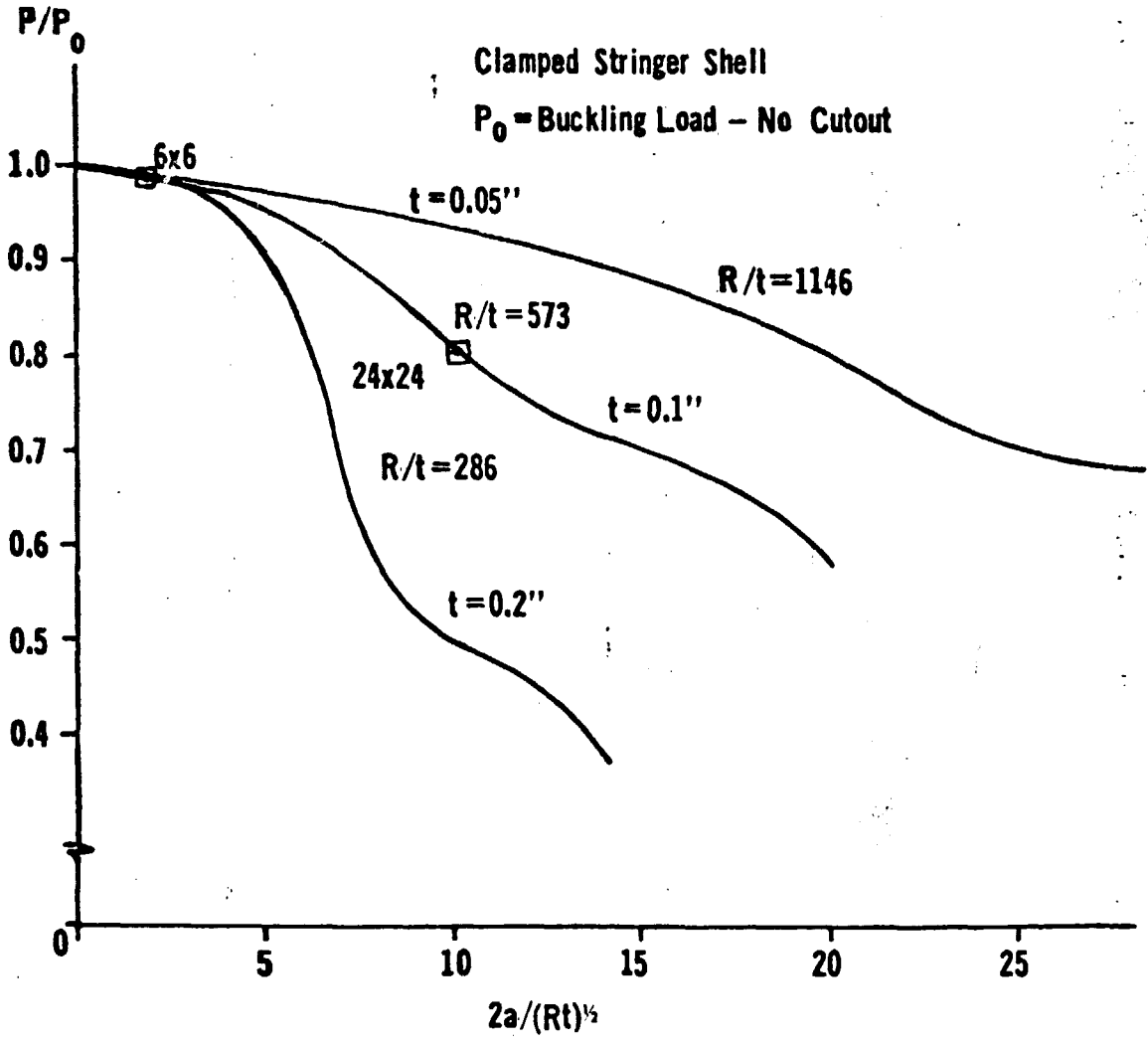

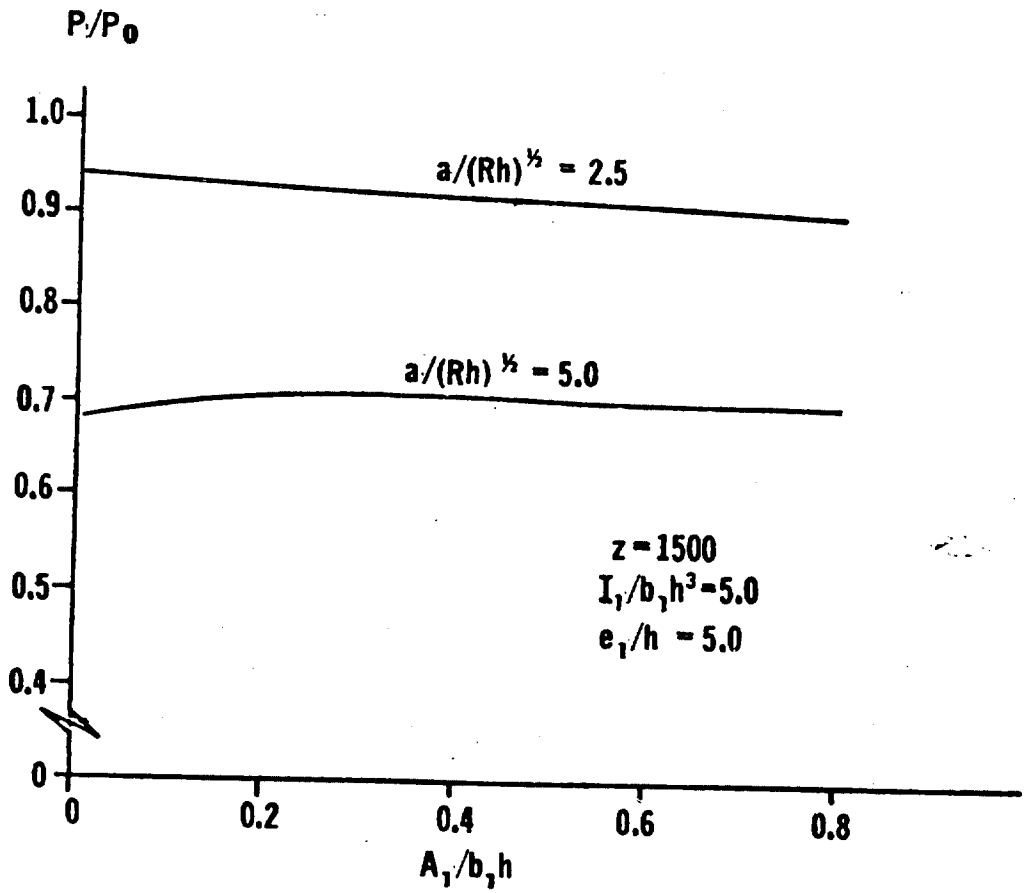
P/P0
1.0
0.9
0.8
0.7
0.6
0.5
0.4
0
a/(Rh)½ = 2.5
a/(Rh)½ = 5.0
z = 1500
I1/b1h3 = 5.0
e1/h = 5.0
0
0.2
0.4
0.6
0.8
A1/b1h

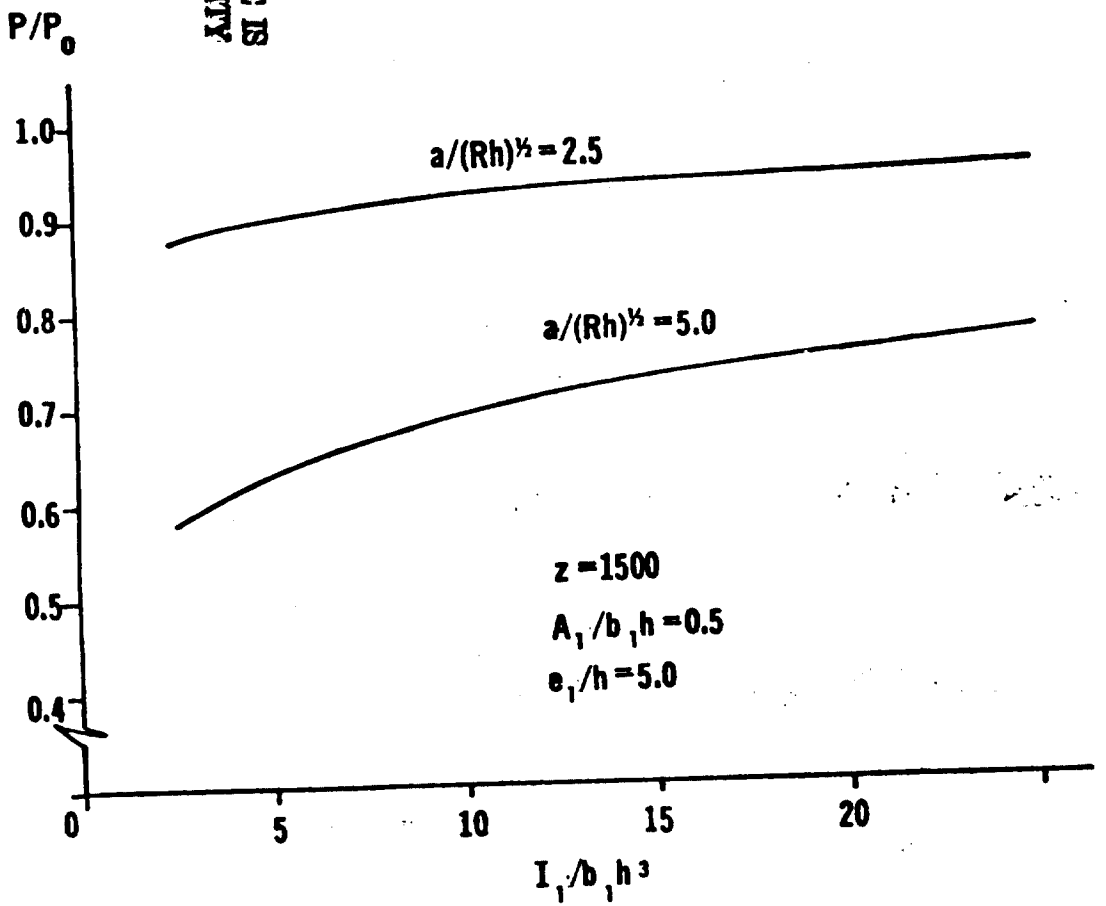

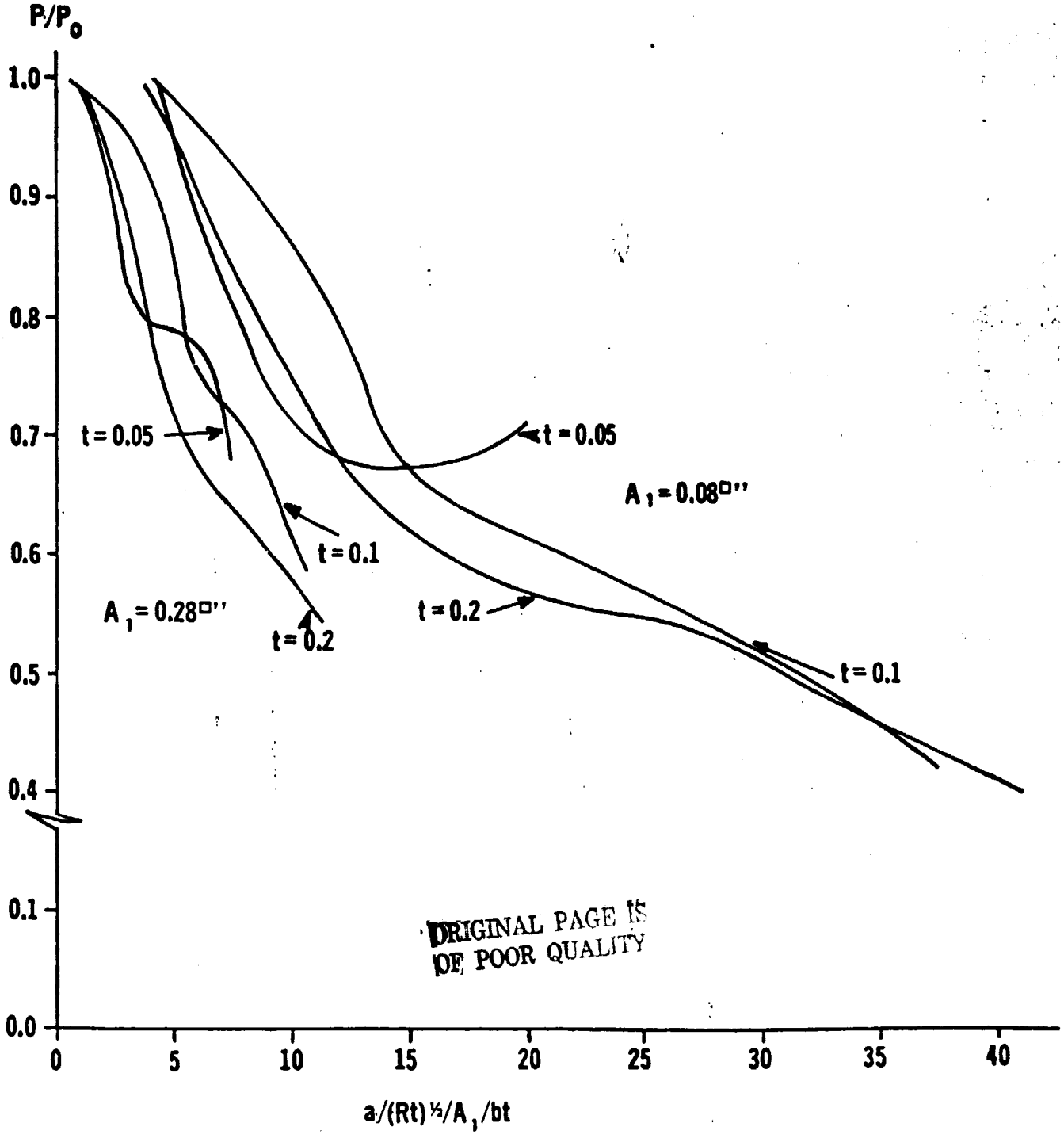

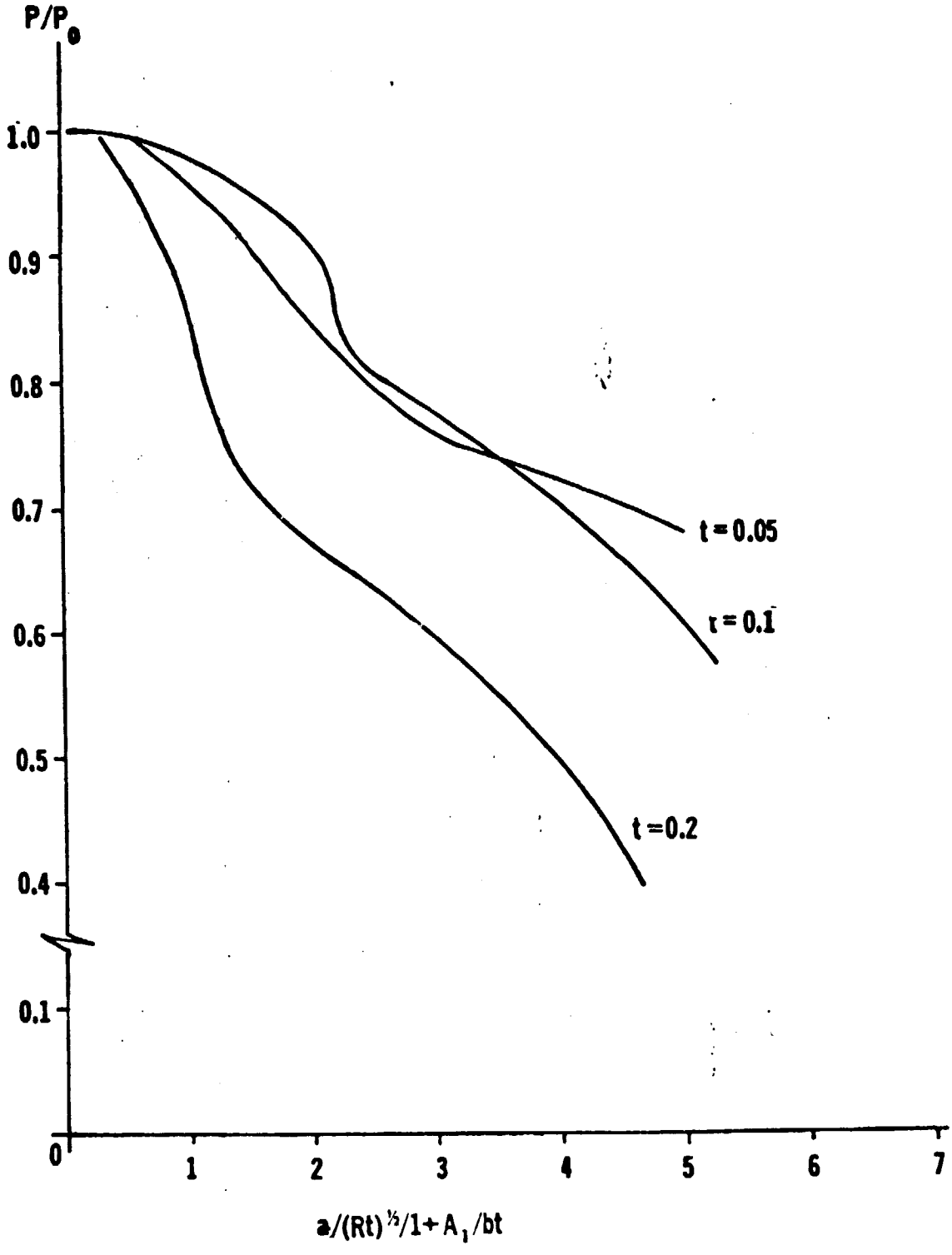
P/P0
1.0
0.9
0.8
0.7
0.6
0.5
0.4
0.1
0
1
2
3
4
5
6
7
t = 0.05
t = 0.1
t = 0.2
a/(Rt)½/1+A1/bt

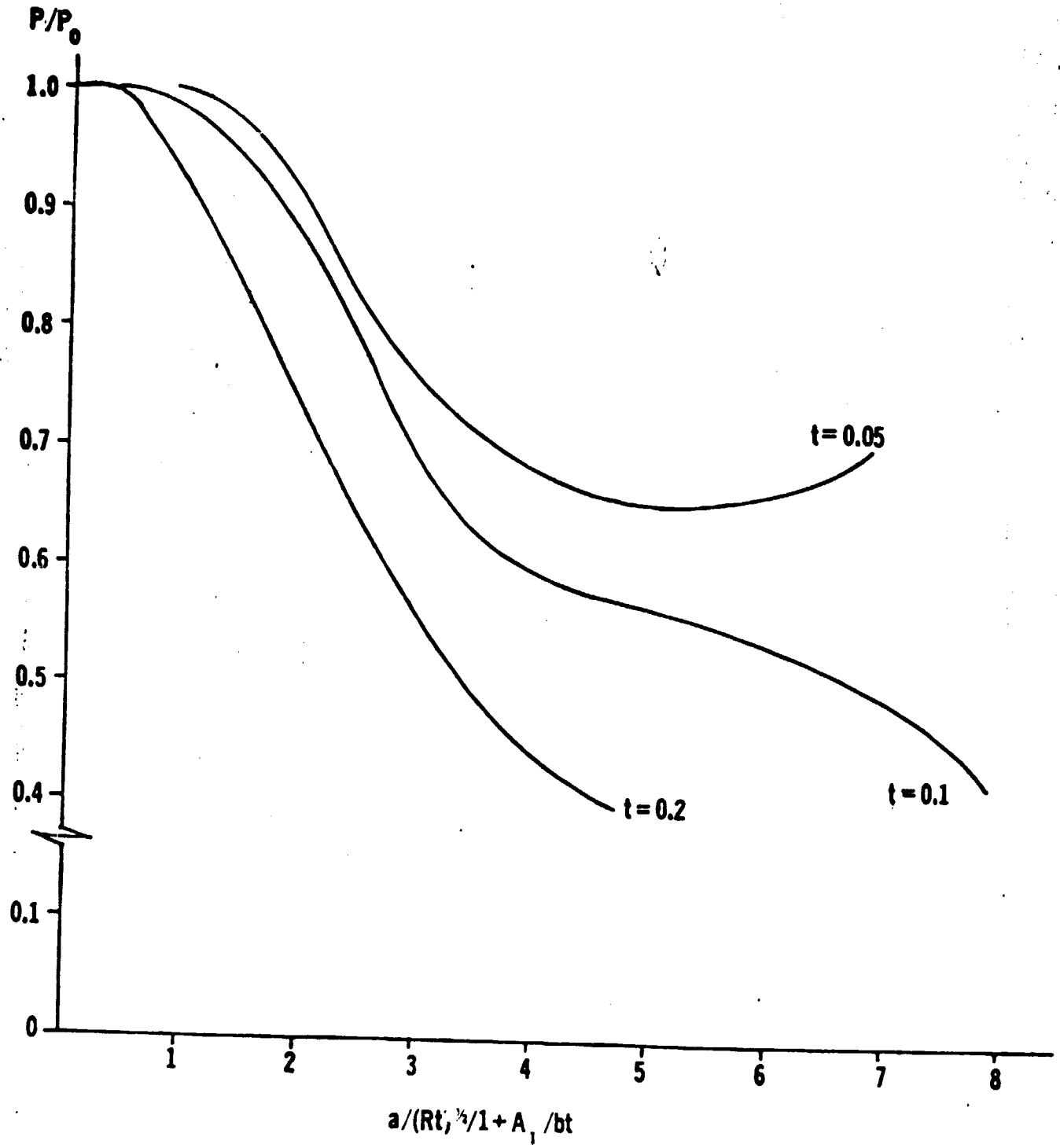
P/P0
1.0
0.9
0.8
0.7
0.6
0.5
0.4
0.1
0
t = 0.05
t = 0.2
t = 0.1
1
2
3
4
5
6
7
8
a/(Rt)^½/1 + A1 /bt

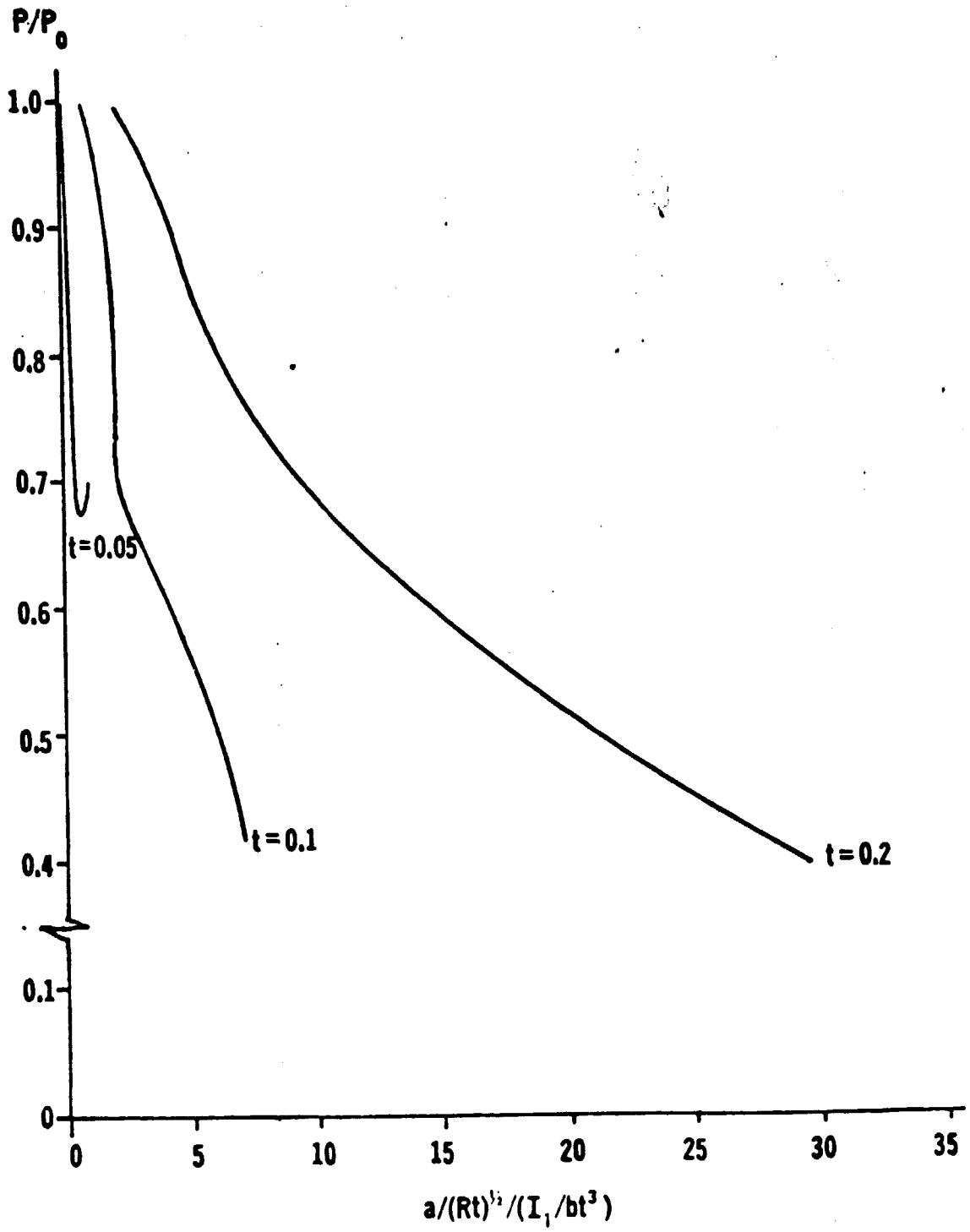
P/P0
1.0
0.9
0.8
0.7
0.6
0.5
0.4
0.1
0
t=0.05
t=0.1
t=0.2
0
5
10
15
20
25
30
35
a/(Rt)^½/(I1/bt^3)

Fig. 2.5

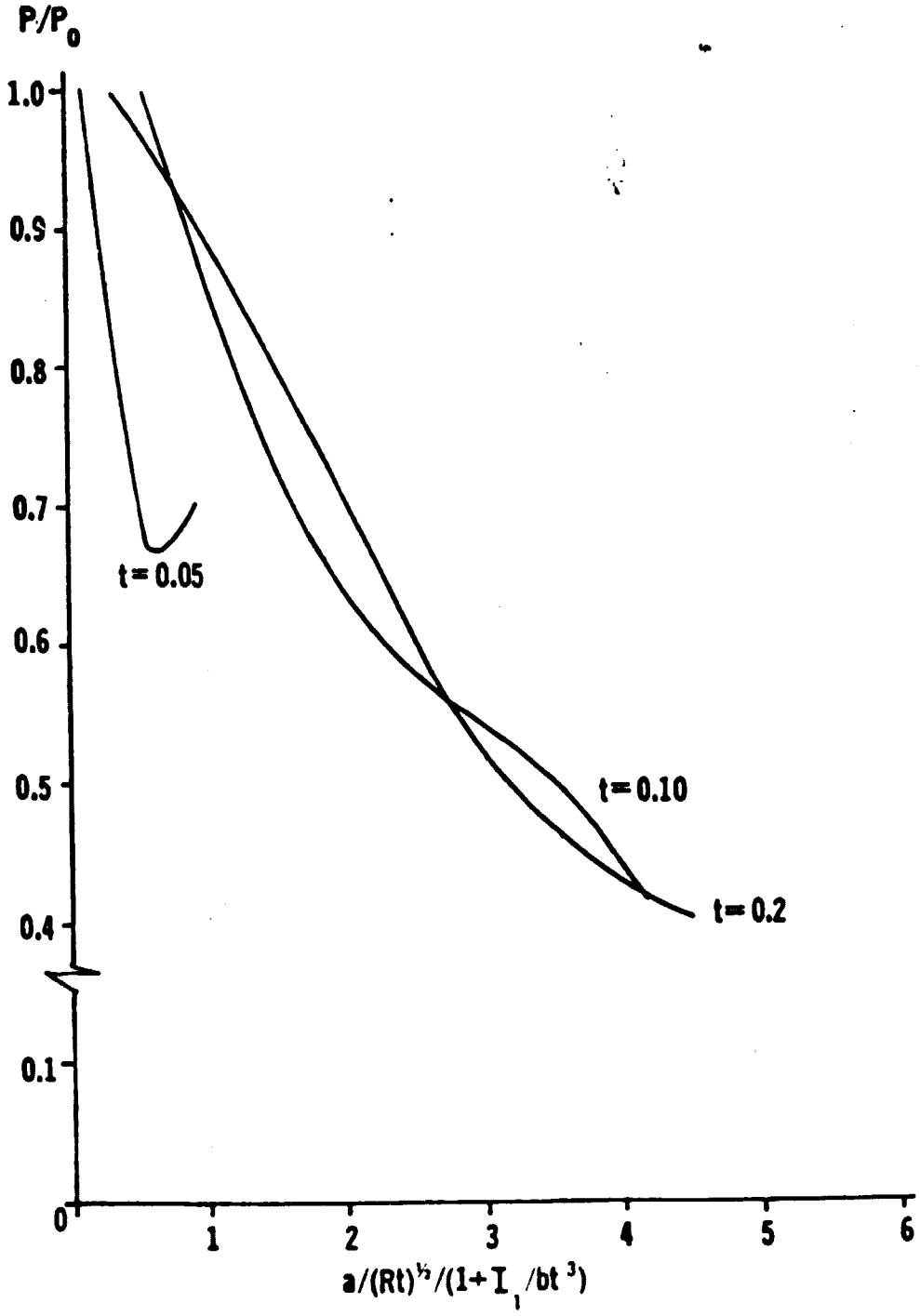
P/P0
1.0
0.9
0.8
0.7
0.6
0.5
0.4
0.1
0
t = 0.05
t = 0.10
t = 0.2
1
2
3
4
5
6
a/(Rt)½/(1+I1/bt3)

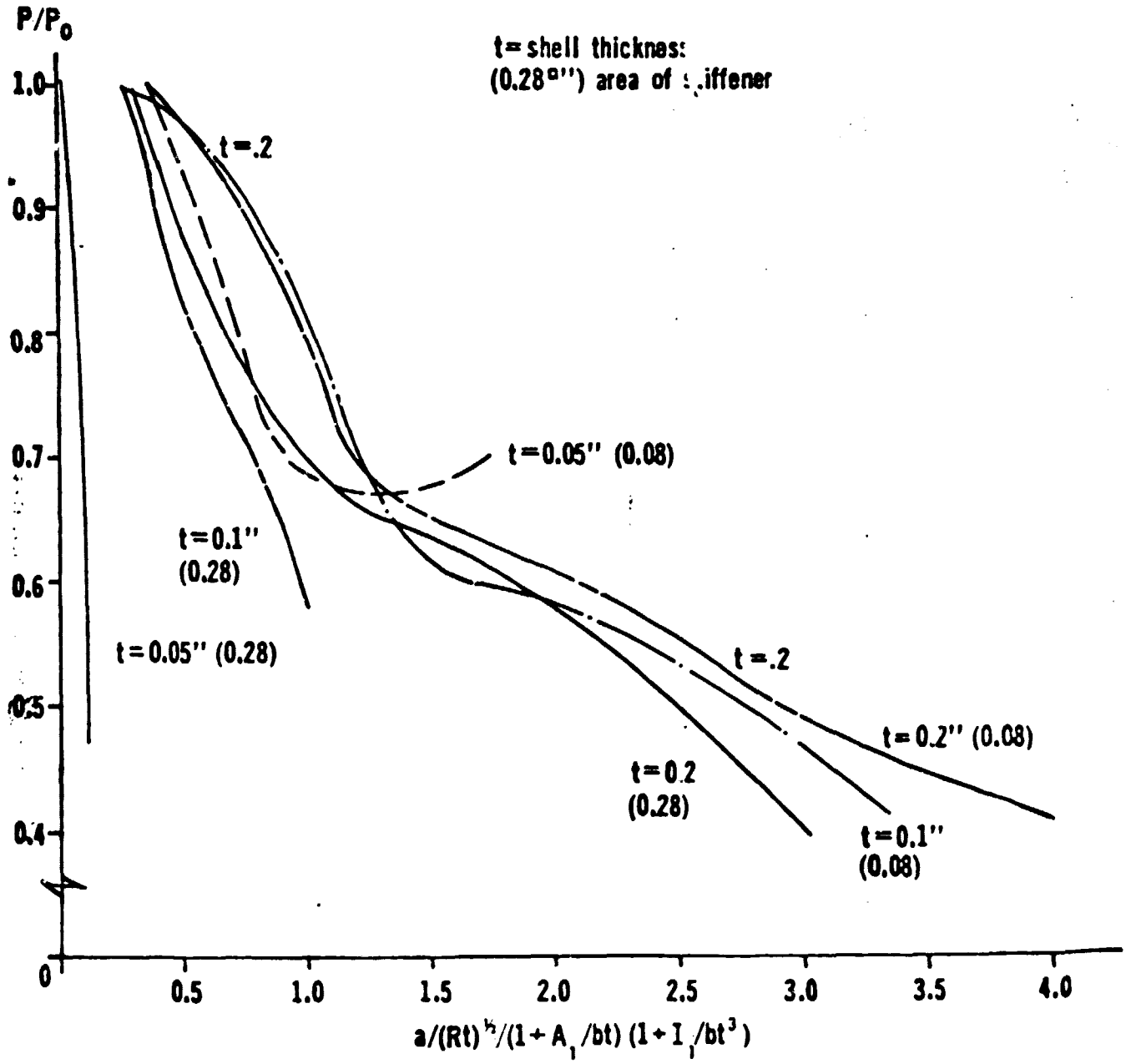

Fig. 2